Granular Matter (2011) 13:319–340
DOI 10.1007/s10035-010-0229-0

ORIGINAL PAPER

Seismo- and thermodynamics of granular solids

Gerd Gudehus · Yimin Jiang · Mario Liu

Received: 6 May 2010 / Published online: 4 November 2010

Abstract The recently published theory named Granular Solid Hydrodynamics (GSH) is outlined, supported and quantified with arguments from physics as well as soil mechanics. Seismodynamic equilibria serve to introduce a granular temperature T_g and a related entropy s_g, both with gradients. The evolution equations of GSH are first presented without gradients, parameters are proposed as functions of T_g and estimated. Constant stretching leads to nearly hypoplastic relations for a certain range of T_g. Cyclic deformations lead to pulsating T_g and to asymptotic cycles of stress and density. State cycles are also attained with additionally imposed isochoric deformations (ratcheting). Similar attractors can be obtained with elastoplastic or hypoplastic relations with hidden variables. GSH is then presented with gradients and boundary conditions. Consequences for stabilization and destabilization are outlined by means of the total energy and with driven attractors. Conclusions and an outlook indicate that GSH is going to become a powerful unified concept.

Keywords Hydrodynamics · Thermodynamics · Constitutive relation

G. Gudehus
Emeritus, Institute für Bodenmechanik und Felsmechanik, University Karlsruhe, Karlsruhe, Germany

Y. Jiang
Central South University, Changsha, China

M. Liu (✉)
Institut für Theoretische Physik, University Tübingen, Tübingen, Germany
e-mail: mliu@uni-tuebingen.de

1 Introduction

In TA ΦΥΣΙΚΑ, the first ever book on physics, Aristoteles defined the difference of continuous and granular matter by the response to $\epsilon\nu\acute{\epsilon}\rho\gamma\epsilon\iota\alpha$ (noticed by Th. Triantafyllidis). This was not energy in a modern sense, but action, probably *seismic* (i.e. shaking). The micro-seismicity of deformed or shaken *granular solids* (in the sense of [1]) resembles thermal oscillations, but its energy is not stored like heat, as granular interaction is not conservative. The word *seismodynamics* was coined for the counterpart of thermodynamics which is needed in addition for granular solids.

Maxwell remarked that sand has a "historical element," therefore it eludes mathematical treatment in the opinion of Darwin [2]. The mechanical behaviour of hard-grained soils is in fact astonishingly complex. Engineers tried to catch it by means of stiffness and strength, but rather in vain. Elastoplastic and hypoplastic constitutive relations work for certain deformations, but with repeated reversals anelastic effects are thus grossly under- or overestimated, respectively. Models of both kinds can be more realistic with hidden variables, but they are then intricate and physically obscure. Viscous effects are usually neglected for hard grains although they were observed [3]. Such models were applied in boundary value problems, but the partial validation by observations is not clear and the energetics is not captured explicitly.

One of us (G.G.) proposed to escape from "a morass of equations and a jungle of data" in a forthcoming book (Physical Soil Mechanics, 2010, PSM in the sequel) by means of *attractors*. These are first meant experimentally for uniform so-called elements as the asymptotic response to certain deformations, and theoretically for constitutive models which can thus be validated and calibrated. Constant stretching, i.e. proportional deformation, causes a gradual determination of hidden states by stress, this was called *swept-out of*

memory (SOM, [4]). With continued monotonous stretching elements approach *state limits*, for which the void ratio e is determined by the mean pressure p and the ratio $\tan \psi_s$ of mean shear stress $\bar{\tau}$ and p. Among these attractors so-called critical states are distinguished by stationary $e = e_c(p)$ and $\tan \psi_s = \tan \psi_c$. Contractant stretching leads to $e > e_c$ with $\tan \psi_s < \tan \psi_c$ up to grain crushing, dilatant stretching leads to $e < e_c$ with $\tan \psi_s > \tan \psi_c$ up to decay. The desired uniformity of elements gets lost with the approach to state limits.

As far as grain crushing and decay can be avoided cyclic deformations lead to *state cycles* asymptotically, with higher harmonics in case of harmonic stretching. State cycles are also obtained with superimposed isochoric stretching (ratcheting). Observed asymptotic stress cycles are fairly well reproduced by certain elastoplastic and hypoplastic relations with hidden variables (PSM). The latter could represent the force-roughness of the grain contacts, with more marked force chains in case of bigger amplitudes. Cyclic deformations with minute amplitude can lead to an almost hypoelastic (i.e. stress-dependent elastic) response, whereas ratcheting implies more dissipation due to the average stretching.

To a certain extent validations and calibrations can be achieved with these attractors, but there are limitations. Localized shearing and collapse confine the desired uniformity of 'elements' , strange attractors for such granular phase conditions are not yet at hand. They can be avoided with smaller amplitudes between reversals, but with many of them numerical simulations get uncertain and expensive. So-called seismo-hypoplastic relations were proposed for cumulative anelastic effects [5] with a heuristic *granular temperature* T_g instead of the temperature T which matters (PSM) in Niemunis' [6] visco-hypoplasticity. T_g can get stationary for monotonous average deformations, and can pulsate otherwise with an imposed frequency. Some experimental results could thus be matched, but the energetics remained obscure.

Attempts of this kind are not new in geotechnical engineering. Barkan [7] proposed a 'vibro-viscosity' and a reduced strength of shaken dry sand. Triantafyllidis (unpublished) estimated the vibration-induced granular flow towards an excavation with a T_g-dependent viscosity. More recently he proposed the field equation

$$T_g = s \nabla_i^2 T_g \tag{1}$$

by means of Valanis' et al. [8] *granular entropy* S_g. One of us (G.G) derived (1) from the balance of seismic relaxation and diffusion. Equation (1) is thought for stationary shaking with stationary average state and shape. It was not possible to validate attempts with athermal T_g and S_g as proposed by Valanis et al. [8], Herrmann [9], Edwards and Oakeshott [10] and Kondic and Behringer [11]. T_g causes heat production so that T can only get stationary for continuous shaking, and exhibits gradients $\nabla_i T$. More generally speaking, *seismodynamics requires thermodynamics*.

There is now a thermodynamically based, general and rigorous approach to macroscopic description. The resulting theories are usually referred to as *hydrodynamic* by condensed matter physicists. This attribute will also be employed here, with the needed clarification (and some trepidation, as it may lead to misunderstanding among engineers). The hydrodynamic approach was developed over the years by many people, but one may probably take it to have been proposed and developed by see Landau and Lifshitz [12,13] and Khalatnikov [14] to understand superfluid He^4, see also de Groot and Masur [15] and de Gennes and Prost [16]. One of us employed this approach to account for ferrofluids [17,18] and polymers [19,20]. This was carried over, together with a second of us, to granular matter, in spite of some obvious difficulties constructing a hydrodynamic theory for granular media [21]: At first, static granular matter was considered employing a "stress-elastic strain relation," derived from an appropriate elastic energy [22–24]. Extending the hydrodynamic approach with a granular entropy s_g and the associated temperature T_g, hypoplastic relations were then obtained for monotonous deformations with a stationary T_g [25]. Finally, this approach was generalized to GSH (for *Granular Solid Hydrodynamics*) [26,27]. Compared with other matter, GSH, especially the specification of its parameters, is fairly intricate, though we do hope that the arguments presented here will help the reader to understand its essence and realize its potential.

Section 2 starts with thermodynamic equilibria and goes on with seismodynamic ones. T_g and s_g are related via the seismic energy, and (1), employed in a well-defined sense, is given a more complete form. GSH-equations without gradients are introduced in Sect. 3, parameters are specified as functions of T_g. The attractors indicated further above can thus be reproduced. GSH with gradients is the topic of Sect. 4, which deals also with boundary conditions and the gain or loss of stability. Notations are taken over from GSH, and water is first left aside. The paper ends with stating in Sect. 5 what has been and what could further be achieved.

An "Appendix" is provided at the end of this paper that contains all GSH equations, made dimensionless and appropriate for numerical simulations of triaxial tests.

2 Equilibria

2.1 Thermodynamic equilibria

Assemblies of hard grains with gravity can stay at rest, enabling an elastic solution. Being *jammed*, the grains transfer normal and shear stresses as in a solid, with elastic deformation and energy. They can be differently packed, but there are upper and lower bounds for the void ratio e. Similar to an elastic solid, the stress field is determined by equilibrium and

boundary conditions, though with the difference that the density is an independent variable in granular media and needs to be specified. When Maxwell stated that 'sand when put together in different ways would exercise different thrusts' [2], he referred to the observation that granular stresses are not determined by the strain alone. A granular system sustaining a static elastic solution is in a stable thermodynamic equilibrium.

Leaving aside polar effects, average grain contact forces can be represented by the field of negative Cauchy stress σ_{ij} (sign convention of soil mechanics). In equilibrium, this equals the elastic stress π_{ij}. With constant grain density ρ_s the overall density is $\rho = \rho_s/(1+e)$. The void ratio e ranges between bounds which depend on the mean pressure $p = \pi_{ii}/3$. This can be scaled by a granulate hardness h_s (PSM). e-bounds decrease with p near $p = 0$ by a power law [28],

$$e_0 - e \propto \left(\frac{p}{h_s}\right)^n . \tag{2}$$

Often, $n \approx 1/2$ suffices. $e \to 0$ is thus not obtained for $p \to \infty$, and also impossible due to grain crushing. An upper bound e_i is approached by isotropic compression of loose grain skeletons which tend to collapse. Elastic solutions remain static only for $e < e_i$, they are unstable for higher porosity, when grains necessarily flow. A lower bound e_d is approached by cyclic deformations with constant p. For critical states $e = e_c$ lies somewhere between e_d and e_i.

Limit void ratios for a given p can be related with the stress obliquity $\tan\psi_s = \bar{\tau}/p$ for state limits (spatially averaged shear stress $\bar{\tau}$). Uniform state limits are not attainable as they are unstable, but monotonous deformations can lead close to them (PSM). Near the upper bound e_i grain skeletons collapse under isotropic pressure, this means a loss of energetic stability by the elastic solution, possibly via a chain reaction. Conventional critical states have a p-dependent e_c and a critical obliquity $\tan\psi_{sc}$ which can be substituted by a critical friction angle φ_c. They are defined as steady states for stationary isochoric stretching (constant volume), but typically cannot be attained uniformly with elements.

So-called peak states with overcritical obliquities ($\tan\psi_s > \tan\psi_{sc}$) can be approached with $e < e_c$ and dilatant stretching, in particular with $p = \text{const}$ (isobaric). Samples with such states can be kept at rest by means of fixed plates, but observed patterns of shear bands indicate that the uniformity desired for elements is no more given (PSM). This means that uniform elements are unstable for given pressure and overcritical mean shear stress, and dilate along shear bands the more marked the lower $e < e_c$ is. Critical states and shear bands are being actively considered at the moment employing GSH. The results will be reported elsewhere.

The elastic deformations of jammed hard grains sum up to a small *elastic strain* u_{ij} (extension positive). The specific elastic energy w_e is a function of u_{ij} and density ρ (or e). Its total differential for neighbored states is $\mathrm{d}w_e = -\pi_{ij}\mathrm{d}u_{ij}$ for constant ρ, this means

$$\pi_{ij} = -\left.\frac{\partial w_e(u_{k\ell},\rho)}{\partial u_{ij}}\right|_\rho \tag{3}$$

as for solids. This is thermodynamically correct for spatial averages of grain ensembles although actual strains of granular solids are never purely elastic. Other than with an elastic solid the density ρ is an independent variable. The total differential of w_e is therefore $\mathrm{d}w_e = \mu\mathrm{d}\rho - \pi_{ij}\mathrm{d}u_{ij}$, with a chemical potential

$$\mu = \partial w_e/\partial\rho|_{u_{ij}} \tag{4}$$

that, with $||u_{ij}|| < 10^{-3}$ for hard grains, may often be neglected, $\mu \ll \pi_{\ell\ell}/\rho$.

w_e vanishes for $p = 0$ and increases with p by a power law near $p = 0$. It must be a locally convex function of u_{ij} and ρ, otherwise energy would be released by suitable $\mathrm{d}u_{ij}$ and $\mathrm{d}\rho$. A *stability limit* with respect to π_{ij} is given by dry friction independently of ρ. This can be seen with a thin granular layer between an inclined rough plate and a movable plate with weight. It cannot stand with any ρ if the slope angle β is more than critical, i.e. with $\tan\beta = \tau/p > \tan\varphi_c$. Grain skeletons are also unstable at the upper e-bound with isotropic pressure, i.e. for $e = e_i$ and $\pi_{ij} = p\delta_{ij}$, then a collapse indicates another verge of convexity of the energy function (i.e. its differential is just no more a positive definite quadratic form). As outlined with a thin layer uniform grain skeletons cannot stay at rest with overcritical obliquities $\tan\psi_s$ as then w_e is no more stable with respect to u_{ij}. Shear bands observed with overcritical $\tan\psi_s$ and fixed boundaries are often considered including polar quantities (PSM). This may not be necessary within the framework of GSH, and will be considered in a forthcoming publication.

Jiang and Liu [22, 23] proposed the representation

$$w_e = B\sqrt{\Delta}\left(\frac{2\Delta^2}{5} + \frac{u_s^2}{\xi}\right) \tag{5}$$

where $B = B(\rho)$, $\Delta \equiv -u_{ll}$, $u_s^2 = u_{ij}^0 u_{ij}^0$ and $u_{ij}^0 = u_{ij} - u_{ll}\delta_{ij}/3$. Equation (5) with (3) yields

$$\pi_{ij} = \sqrt{\Delta}\left(B\Delta\delta_{ij} - 2Au_{ij}^0\right) + \frac{Au_s^2\delta_{ij}}{2\sqrt{\Delta}} \tag{6}$$

with $A = B/\xi$ and a friction coefficient ξ. A third invariant of u_{ij} is of higher than the given order in the strain field, and omitted in (5) for simplicity. But we do expect it to be significant, especially for turning the yield surface from Drucker-Prager to a Mohr-Coulomb-type one. w_e by (5) is no more stable (i.e. convex) for $u_s/\Delta \geq \sqrt{2\xi}$, i.e. with (6) if the friction condition

$$\frac{\pi^0_{ij}\pi^0_{ij}}{p^2} = \frac{2}{\xi} \tag{7}$$

holds. The chosen $\xi \approx 5/3$ corresponds to a rather small critical friction angle $\varphi_c \approx 28^0$. A third invariant would influence φ_c (PSM). Factor B replaces h_s in (2) for scaling of pressures, it can likewise reach almost 10 GPa for round quartz grains. With these quantities the elastic energy $w_e \approx (2/5)B(p/B)^{5/3}$ is about 20 Nm^{-2} for a mean pressure $p = 100$ kPa and a volumetric strain $\Delta \approx (p/B)^{2/3} \approx 10^{-3}$. One could include a density dependence of ξ such that the friction angle vanishes approaching the loosest possible density.

A dependence of B on density ρ was chosen so that the hypoelastic stiffness by (3) suits to observations [25]. A more elaborate representation of w_e was proposed by Jiang and Liu [26,27] such that the expression of Eq. (5) turns concave and unstable with respect to ρ for isotropic pressures. We leave aside the algebraic expressions in favor of a discussion with physical arguments. A verge of convexity of w_e means that its second-order change vanishes for a certain set of elastic strain u_{ij} and density ρ and differentials of both. The latter constitute an eigenvector which is not elastic in general as elastic changes of ρ can be much smaller than density changes by rearrangement. A change of state in this direction at the verge of convexity would lead to localization with new degrees of freedom.

At the verge of stability, the system enters a state limit as described in PSM. State limits imply a unique dependence of void ratio e (which is equivalent to ρ) on mean pressure p and stress obliquity $\tan\psi_s$. This can also be considered employing GSH, results will be reported soon. For the moment, we note that state limits can be approached but not reached by GSH describing monotonous deformations. In the vicinity of state limits, GSH properly accounts for an e-dependent $\tan\psi_s$ and a related direction of stretching, with appropriate eigenvector $\dot{u}_{ij}$ and $\dot{\rho}$ (Sect. 3.4).

Uniform states of rest as in perfect granular samples are stable if they do not release seismic energy spontaneously with growing fluctuations. Otherwise samples exhibit an increase of the granular temperature T_g until they find a new thermodynamic equilibrium with $T_g = 0$. Such a loss of equilibrium depends on boundary conditions and is accompanied by a loss of uniformity: deformations localize into narrow bands which dilate for lower than critical e and contract otherwise (compaction bands).

2.2 Seismodynamic equilibria

Imagine a vessel filled with dry sand and shaken continuously so that the grains are never at rest. After a transition, which takes longer for weaker shaking, the sand has a horizontal free surface and does not flow any more on average, its pressure p is hydrostatic and its density is close to the upper bound ρ_d (except for granular boiling which is treated further below) [29]. Such *seismodynamic equilibria* are attractors, i.e. the state field for a given mass of sand, shape of vessel and kind of stationary shaking is attained with any initial shape and state and not changed with stationary boundary conditions. Similar states are attained in the near-field of vibrators, they are no more influenced by the far-field. The attained hydrostatic pressure enhances driving or floating of solid bodies and can break silos designed for lower Janssen-pressures.

The grains get unjammed in the transition so that the elastic energy w_e vanishes at seismodynamic equilibria. The granular matter still has specific seismic energy w_s, thermal energy w_t and gravitational energy w_g, and the energy density $w_{tot} = w_s + w_g + w_t$ is integrated minimal with respect to other shapes and states. The heat-like seismicity is captured in GSH by a *granular temperature* T_g. The ordinary temperature T tends to a stationary field which is determined by the balance of thermal energy (Sect. 4.1). Formally speaking, same as T and s for thermodynamic equilibria, T_g is the conjugate variable to s_g, the *granular entropy*, i.e.,

$$T \equiv \left.\frac{\partial w_s}{\partial s}\right|_{\rho,T_g}, \quad T_g \equiv \left.\frac{\partial w_s}{\partial s_g}\right|_{\rho,T}, \tag{8}$$

where the specific *seismic energy* w_s depends also on the density ρ. The change of heat and heat-like seismic energy is therefore written as

$$T\,\mathrm{d}s + T_g\,\mathrm{d}s_g. \tag{9}$$

During a relaxation of T_g, energy is transferred from $T_g\mathrm{d}s_g$ to $T\,\mathrm{d}s$. The granular temperature can easily attain values similar to the Sun's internal temperature, $T_g \gg T$. But we also have $\mathrm{d}s_g \ll \mathrm{d}s$, as there are far more molecular than granular degrees of freedom. The loss of seismic energy is equal to the gain in thermal energy in case of seismodynamic equilibrium: $T_g\mathrm{d}s_g + T\,\mathrm{d}s = 0$.

T_g and s_g vanish in states of rest as both are seismic. This is achieved with $w_s \propto s_g^2 \propto T_g^2$ being a minimum with respect to s_g or T_g at $T_g, s_g = 0$. This way, stable systems, when unperturbed, automatically return to $T_g = 0$. A linear dependence $w_s \propto T_g$, is only appropriate for the rarefied and high T_g range, not the high density and low T_g limit under consideration here. Assuming that w_s—a kinetic-like energy including fluctuating elastic fractions—is proportional to ρ, one can write

$$w_s = \frac{s_g^2}{2b\rho} = b\rho\frac{T_g^2}{2} \tag{10}$$

with a factor b which depends on the relative density ρ/ρ_d with an upper bound ρ_d (more below). Equation (8) and (10) imply

$$s_g = b\rho T_g. \tag{11}$$

$w_s \propto s_g^2$ by (10) is also needed for the stability of seismodynamic equilibria with T_g near 0 [26,27]. Only when the density is much lower, in the granular gas state, does the dependence become $w_s \propto T_g$ [30].

Seismic energy is continuously transformed into heat at the grain contacts, this is expressed in the simplest possible way by a relaxation term

$$\frac{\partial s_g}{\partial t} \equiv \dot{s}_g = -\gamma \frac{s_g}{b\rho}, \tag{12}$$

with a *quiescence factor* γ which depends on T_g (as will be outlined in Sect. 3.1), a factor b as in (10) and the density ρ. If this *relaxation of seismicity* is counter-balanced by the diffusive flow of granular entropy,

$$t_i \equiv \chi^2 \nabla_i \frac{s_g}{b\rho} = \chi^2 \nabla_i T_g \tag{13}$$

with a diffusion factor χ^2, we have

$$T_g - \nabla_i t_i = T_g - \chi^2 \nabla_i^2 T_g = 0, \tag{14}$$

which agrees formally with (1) and may likewise be interpreted as the balance of seismic power at seismodynamic equilibrium. It means stationary gradients of T_g and requires a specification of T_g along boundaries, which may be called *seismostats* in analogy to thermostats with given T. Seismic energy enters a granular body from shaking boundaries at the same rate as it is transformed into heat at grain contacts and radiated off into neighbored bodies.

The factor b in (10) depends on the density ρ as [26, 27]

$$b = b_0(1 - \rho/\rho_d)^a, \tag{15}$$

with a constant b_0, an exponent $a \approx 0.1$ and the upper bound ρ_d as introduced above, in Sect. 2.1. The *seismic pressure* is thus

$$p_T = -\frac{\partial w_s/\rho}{\partial(1/\rho)} = \frac{\rho}{2\rho_d} \frac{a\rho b_0 T_g^2}{(1-\rho/\rho_d)^{1-a}}. \tag{16}$$

as the seismic energy w_s for seismodynamic equilibria decreases uniquely by a density increase due to a higher pressure with constant T_g. The small exponent a expresses the known minute pressure-dependence of density by shaking. The factor b_0 is so small that p_T compensates gravity only with ρ very near ρ_d for the range of T_g where one may speak of granular solids.

Granular boiling serves for estimating two parameters and for illustrating a limitation of GSH by transition to a granular fluid. For instance, dry fine sand in a vessel upon a vibrator boils up with convection cells by means of about $100\,\mathrm{s}^{-1}$ frequency and ca. 1 mm amplitude at the base. At this transition the seismic energy w_s is proportional to T_g, thus the granular temperature T_g is $T_b \approx 10^9$ K from $mv^2 = k_B T_g$ (grain mass m, grain velocity v, Boltzmann constant k_B) for the base of our vessel. The interpolation

$$w_s \propto \frac{T_g}{T_b}\left(1 - \exp\left(-c\frac{T_g}{T_b}\right)\right) \tag{17}$$

gets almost linear for $T_g \approx T_b$ (fluid-like) with $c \approx 7$, and agrees with (10) for $T_g \ll T_b$ (solid-like). This leads to $b_0 \approx 10^{-19}\,\mathrm{m}^2/(\,\mathrm{s}^2\mathrm{K}^2)$ for the investigated sand, which suffices in the sequel to neglect w_s and p_T against other energies and pressures, respectively. Thus the granular entropy s_g by (11) with (15) is far lower than the thermal one, as proposed with (9). Other interpolations than (17) lead to similar w_s and p_T, a more precise value of b_0 is not yet needed. The diffusion factor χ in (14) can be estimated from the indifference of the specific energy $w_s + w_g$ above the shaking base: as a diffusive reduction of seismic energy w_s is compensated by a gain of gravitational energy w_g a boiling sand has no more a single configuration with a minimal free energy. This leads to $\chi \approx 0.1$m for dry fine sand, an estimate which suffices in the sequel.

It is important to realize that the above estimates, although the best we have, are far from rigorous. The energy in the granular solid phase being $w \sim b_0 T_g^2$, we may approximately equate it with the kinetic energy of the grains in a unit volume, but would still not know what T_g is, as b_0 is unknown. There is always the freedom to make b_0 larger and T_g^2 smaller, or vice versa. The above estimate of b_0 makes the assumption that the energy of a grain in the gaseous phase is $k_B T_g$, with the known coefficient k_B. Interpolating between these two limits, one can estimate b_0 over k_B.

There are two problems with this approach. First, thermodynamics prescribes an energy that is a function of entropy density, $w = w(s_g)$, with the temperature given as a derivative. Then, the seismic energy in the gaseous phase is $w \sim t_0 \ln s_g$, containing an unknown coefficient t_0. An interpolation would relate b_0 to t_0, but cannot deliver its value. Second, if granular boiling has any similarity to a phase transition, it will display discontinuities in the state variables, forbidding a smooth interpolation.

The *partition of seismic energies* w_s can as yet only be guessed. It is stationary for seismodynamic equilibria like other state variables as long as the granular wear may be neglected. Except for grains along harmonically shaken solids no translational granular degree of freedom is preferred, otherwise seismostats could not produce a temperature-like T_g. With ongoing dissipation of granular excitation, perfect equipartition, including rotational and elastic degrees of freedom, is rarely reached in cases considered below. Fortunately, neither does the validity of GSH hinge on it, as GSH treats s_g as a macroscopic and slowly relaxing variable, not necessarily in perfect analogy to the true temperature. What GSH does is only to assume a two-step irreversibility – first in

producing s_g from mechanical energy, then in converting s_g into s, the true heat.

3 Uniform evolutions

3.1 Evolution equations

We confine ourselves in this section to uniform "elements" with hard grains. The *thermal entropy production* in GSH, $\dot{s}$, is given with the rate of dissipation R [cf. (9)] by

$$T\dot{s} = R = \gamma T_g^2 + \beta \pi_{ij}^0 \pi_{ij}^0 + \beta_1 \pi_{ii}^2 \tag{18}$$

with γ as in (12). For specifying β and β_1, two relaxation times τ and τ_1 are defined by

$$\frac{1}{\tau} = 2\beta A\sqrt{\Delta}, \quad \frac{1}{\tau_1} = 3\beta_1\sqrt{\Delta}\left(B - A\frac{u_s^2}{2\Delta^2}\right), \tag{19}$$

which are assumed to be proportional to T_g, with two density-dependent proportionality coefficients λ, $lambda_1$,

$$\frac{1}{\tau} = \lambda T_g, \quad \frac{1}{\tau_1} = \lambda_1 T_g, \tag{20}$$

with the *unjamming factors* $\lambda > 0$ and $\lambda > \lambda_1 > 0$ (specified below). Equation (19) with (6) means

$$\pi_{ij}^0 = -\frac{u_{ij}^0}{\beta\tau}, \quad \pi_{ii} = -\frac{u_{ii}}{\beta_1\tau_1},$$

thus (18) can be substituted with (20) by

$$\begin{aligned} T\dot{s} &= R \\ &= \gamma T_g^2 + B T_g \sqrt{\Delta}\left[\frac{2\lambda}{\xi} u_{ij}^0 u_{ij}^0 + \lambda_1 \Delta^2\left(1 + \frac{u_s^2}{2\xi\,\Delta^2}\right)\right]. \end{aligned} \tag{21}$$

The rate of dissipation is thus a positive definite quadratic form in T_g and π_{ij} (or u_{ij}) for $T_g \geq 0$ and (6). γT_g^2 is the rate of dissipation by (10), (11) and (12) due to the loss of seismic energy into heat. The quadratic terms in π_{ij} or u_{ij} stem from the *seismic relaxation* of elastic stress, or strain equivalently, due to the granular temperature. One can show that this term is given simply by $\sigma_{ij} v_{ij}$ for the steady state. The rate of this relaxation is thus proportional to π_{ij} and u_{ij}, respectively, and to T_g by

$$\frac{\dot{u}_{ij}^0}{u_{ij}^0} = -\lambda T_g, \quad \frac{\dot{u}_{ii}}{u_{ii}} = -\lambda_1 T_g. \tag{22}$$

() This means an exponential loss of u_{ij} with time in case of constant T_g up to a seismodynamic equilibrium with negligible u_{ij} (except for ρ close to ρ_d, Sect. 2.2). It implies that T_g has the same effect whether it stems from shaking or other deformations. Similar expressions are obtained with more elaborate representations for w_e, they imply again that there is no relaxation for $T_g = 0$ and hard grains. The ratio of volumetric and deviatoric relaxation times is taken as constant,

$$\frac{\tau_1}{\tau} = \frac{\lambda}{\lambda_1} \approx 10, \tag{23}$$

which means that the volumetric relaxation is weaker than the deviatoric one. Simulations with GSH indicate $\lambda \approx 10^{-6}/(\mathrm{sK})$, i.e. a half-life by (22) from about 10–10^4 s for T_g between 10^5 and 10^2 K, respectively. These estimates cannot substitute calibrations which will be discussed in Sects. 3.2 and 3.3.

The *seismic entropy production* in GSH without gradients is given with the rate of seismic dissipation R_g (cf. again (9)) by

$$T_g \dot{s}_g = b\rho \frac{\mathrm{d}T_g^2}{2\mathrm{d}t} = R_g = -\gamma T_g^2 + \zeta_g v_{ii}^2 + \eta_g v_{ij}^0 v_{ij}^0. \tag{24}$$

The first term denotes the loss of seismic energy into thermal energy, this part of dissipation equals therefore the one in (18) except for the sign. It is proportional to the seismic energy w_s by (10), this suits to the radiation of kinetic energy w_k in an elastic solid with a rate in proportion to w_k. The other terms in (24) are positive definite in the stretching v_{ij} (ie. the gradient of the velocity, see Sect. 4.1) as this feeds the seismic (granular) entropy by the stick-slip of intergranular dislocations. Equation (24) describes the balance of seismic power which is produced by rerrangement with a granular viscosity and consumed into heat. Jiang and Liu [26, 27] expand the three coefficients in T_g,

$$\gamma = \gamma_0 + \gamma_1 T_g, \quad \eta_g = \eta_0 + \eta_1 T_g, \quad \zeta_g = \eta_0 + \zeta_1 T_g. \tag{25}$$

To ensure (in Sects. 3.2 and 3.3) that the system is hypoplastic at elevated T_g, but becomes hypoelastic as $T_g \to 0$, η_0, ζ_0 were set to zero by Jiang and Liu [26, 27], but will be retained here, see the discussion below, after Eq. (38).

The first of (25) combined with (12) means an exponential decay of seismicity for T_g near 0 by

$$\dot{s_g}/s_g = \dot{T}_g/T_g = -\gamma_0/b\rho \tag{26}$$

after a sudden stop of stretching. The observed acoustic emission [31] indicates half-life well below $\tau_g = 0.1$ s, which cannot be measured as testing devices delay the drop of seismicity after a stop of deformation. Imagine a uniform grain skeleton with heat-like seismicity. Erratic seismic pulses travel through chains of grains and are absorbed at grain contacts. A survival length of say 100 grain diameters d_g and a wave velocity $c_s \approx 10^2$ m/s (say) means $\tau_g \approx 100\, d_g/c_s$, e.g. $10^2.10^{-4}/10^2 = 10^{-4}$ s for fine sand. With $\rho \approx 2\,\mathrm{kN\,s^2/m^4}$ and $b \approx b_0$ as given in Sect. 2.2 this leads to $\gamma_0 \approx b_0\rho/\tau_g \approx 10^{-11}\,\mathrm{N/(sK^2m^2)}$.

The relaxation of seismicity after a stop of deformation is faster than by (26) for higher T_g: then the survival lengths

of seismic pulses are shorter as more excited grain contacts absorb more kinetic energy. This justifies the faster than exponential decay by (12) with (25) and a sufficient γ_1, but the latter cannot be observed directly. $\gamma_1 \approx 10^{-13}\,\mathrm{N/(m^2sK^3)}$ may serve as a preliminary guess, more in Sects. 3.2 and 3.3.

The *granular viscosity* η_g cannot be observed directly at low T_g, but there are qualitative arguments for its specification by (25), so the parameters therein have to be calibrated indirectly. $\eta_g \approx \eta_0$ near seismic rest is being successfully employed to capture unlimited monotonous and very slow shear rates and the observed response to minute vibrations near $T_g = 0$ (Sect. 3.1). The increase of η_g with T_g by (25) can be justified for a deformation with constant stretching v_{ij} from $T_g = 0$: the response is first hypoelastic without seismicity, and gets hypoplastic with $T_g \propto |\, v_{ij}\,|$ after a transition (Sect. 3.2). $\gamma \approx \gamma_1 T_g$ holds for the hypoplastic regime so that $\eta_g/\gamma \approx \eta_1/\gamma_1$ is obtained as needed for rate-independence.

The GSH-parameters introduced above can be determined separately only in dedicated experiments. And a combined calibration was not yet achieved, but orders of magnitude can be estimated. Without seismometers for T_g up to almost 10^6 K like thermometers in a wide range of T one can only guess T_g by matching. It appears that T_g reaches about 10^2 K in the nearly hypoelastic regime (Sect. 3.3) and can attain about 10^5 K in the hypoplastic regime (Sect. 3.2). Other than with granular fluids the viscosity factor η_1 by (25) cannot be determined by rheological measurements, an indirect estimate for the hypoplastic regime yields $\eta_1 \approx 10^{-2}\,\mathrm{Ns/(m^2K)}$ (Sect. 3.2). These quantities are admittedly uncommon and preliminary.

The *elastic strain rate* by GSH without gradients is

$$\dot{u}_{ij} = (1-\alpha)v_{ij} - u^0_{ij}/\tau - u_{\ell\ell}\delta_{ij}/\tau_1 \tag{27}$$

with a *transmission factor* α to be specified below. With τ and τ_1 by (20) this can be written

$$\dot{u}_{ij} = (1-\alpha)v_{ij} - T_g\left(\lambda u^0_{ij} + \lambda_1 u_{\ell\ell}\delta_{ij}\right). \tag{28}$$

The first term with $0 \le \alpha < 1$ captures the gain of elastic strain by the average rearrangement, the further terms represent the loss by seismic relaxation. $\alpha = 0$ holds for $T_g = 0$ as then the response is hypoelastic. α saturates at a constant α_h if T_g exceeds a threshold T_h. This can be expressed by

$$\alpha = \alpha_h \tanh \frac{T_g^2}{T_h^2} \tag{29}$$

with $\alpha_h \approx 0.8$ and $T_h \approx 10^2$K. The saturation for $T_g > T_h$ is needed for the hypoplastic range (Sect. 3.2), the quadratic onset enables a nearly hypoelastic response (Sect. 3.3) and rate-independent collapse modes (Sect. 3.4).

As by (22), the second term in (28) means that the rate of seismic relaxation is proportional to T_g. The unjamming factors $\lambda \approx 10^{-6}/(\mathrm{sK})$ and $\lambda_1/\lambda \approx 10$ may be assumed provisionally as indicated further above. The order of magnitude of λ results from observed rates of seismic creep compared with those by (28) and estimated T_g. λ could be calibrated by means of experiments with cyclic deformations, which could also serve to calibrate parameters for γ and η_g (Sect. 3.3).

The *pressure tensor* by GSH without gradients is

$$\sigma_{ij} = p_T\delta_{ij} + (1-\alpha)\pi_{ij} - \eta_g v^0_{ij} - \zeta_g v_{\ell\ell}\delta_{ij} \tag{30}$$

for hard grains. Therein the elastic pressure π_{ij} is given by (3), the seismic pressure p_T by (16), the transmission factor α by (29), and the granular viscosity by (25). The seismic and viscous parts are negligible for small enough shear rates, so that

$$\sigma_{ij} = (1-\alpha)\pi_{ij} \tag{31}$$

holds for slow rearrangements off free surfaces. With α by (29) this means that the Cauchy stress is determined by the elastic stress and the granular temperature. This equation of state is evident for states of rest with $T_g = 0$ (Sect. 2.1), but uncommon otherwise. It means that the seismicity softens the grain contacts so that they do not transmit the elastic stress related with the average elastic deformation, while the seismic pressure p_T is negligible. Imagine a sample of paramagnetic hard grains jammed in a stiff cage that indicates σ_{ij}, and an oscillating electromagnetic field that produces T_g in a short time and maintains it. The grains get first more jammed by shaking with confinement, i.e. π_{ij} rises without immediate rearrangement, so that the observable stress by (31) need not change much although the factor $(1-\alpha)$ can drop to ca. 0.2. The subsequent relaxation with constant T_g via (22) by rearrangement without average deformation takes longer with times in proportion to T_g, which could be used to calibrate λ, and ends at a pressure p_T which is negligibly low except for ρ very near ρ_d.

The thought experiment for explaining (31) may also help to justify the entropy production by (21). The term with T_g^2 was explained already further above. The one with T_g for the heat production by seismic relaxation is due to intergranular pressure and erratic oscillations without average rearrangement (only the latter produces seismicity). The ratio of both parts, roughly $B\lambda\Delta^{5/3}/\gamma T_g$, could principally be estimated by granular-dynamic simulations, whereas λ and γ can only be indirectly calibrated.

In the range wherein (31) holds the thermal energy exceeds the seismic one by far, $w_s \ll w_e < w_t$, so how can the seismic activation matter more then the thermal one? w_s goes over into heat and mobilizes thus a minute fraction of the grain molecules. Luong [32] observed that grain contacts of dry sand get hot temporarily during slow skeleton deformations. This means an activation of contact dislocations by seismic kinks, whereas the average thermal energy is too small to activate dislocations in the bulk of hard grains.

The rate of elastic stress by (3) is

$$\dot{\pi}_{ij} = \mathcal{M}_{ijkl}\dot{u}_{kl} = \left(\frac{\partial^2 w_e}{\partial u_{ij}\partial u_{kl}}\right)\dot{u}_{kl} \tag{32}$$

with the elastic energy w_e by (5) or a better substitute. The rate of the Cauchy stress by (31) is

$$\dot{\sigma}_{ij} = (1-\alpha)\dot{\pi}_{ij} - \dot{\alpha}\pi_{ij}. \tag{33}$$

The evolution equations for elements are completed by

$$\frac{\dot{\rho}}{\rho} = -v_{ii} \tag{34}$$

in case of isochoric grains.

The terms with α in (27) and (31) cancel each other in the entropy production, so the transmission factor α does not appear in the dissipation by (21). The latter is triggered by the balance of seismic power (24), this dissipative detour via heat-like seismicity is a key feature of GSH. Imagine a bicycle with a gear shift. A bigger α implies more pedaling at reduced torque, both with the same factor. The micro-seismicity reduces the transmission by the same factor as the intergranular forces.

The coefficient α is a common example of an off-diagonal element in a Onsager force-flux relation, while those with β, β_1 of Eq. (18) are diagonal ones. Depending on the time reversal properties, the off-diagonal elements are either symmetric or antisymmetric, in either case giving rise to the same magnitude for the coefficients in two evolution equations. This symmetry derives from the reversibility of the underlying, microscopic dynamics and is frequently referred to as the *Onsager Reciprocity Relation*: Starting with the stress and the evolution of shape, written as $\sigma_{ij} = \pi_{ij} - \sigma^D_{ij}$ and $\dot{u}_{ij} - v_{ij} = X_{ij}$, where σ^D_{ij} is the dissipative stress fraction and X_{ij} the anelastic stretching rate, the entropy production is

$$R = \sigma^D_{ij} v_{ij} + X_{ij}\pi_{ij} + \cdots, \tag{35}$$

in addition to other terms that need not be specified here, see [26]. Expanding the fluxes σ^D_{ij}, X_{ij} in the forces v_{ij}, π_{ij}, the Onsager force-flux relations are

$$\sigma^D_{ij} = \zeta\, v_{\ell\ell}\delta_{ij} + \eta v^0_{ij} + \alpha_{ijk\ell}\pi_{k\ell}, \tag{36}$$

$$X_{ij} = \beta\pi^0_{ij} + \beta_1\delta_{ij}\pi_{\ell\ell} + \bar{\alpha}_{ijk\ell}v_{k\ell}, \tag{37}$$

where the Onsager Reciprocity relation prescribes $\bar{\alpha}_{ijk\ell} = -\alpha_{k\ell ij}$. As a result, the α-tensors do not contribute to R, as one can verify by inserting (36, 37) into (35). Taking for simplicity $\alpha_{ijk\ell} = \alpha_{k\ell ij} = \alpha\delta_{ik}\delta_{k\ell}$, we arrive at the relevant terms of (28, 31).

Note that the *viscosities* η, ζ are different from η_g, ζ_g of Eq. (30) and need to be added to them. These here account for the conversion of macroscopic kinetic energy directly into heat and were neglected above for simplicity. Since these would be the only viscosities that exist in a solid or liquid, we may refer to them as the *solid viscosity*.

Taking

$$\eta_0 = 0, \quad \zeta_0 = 0, \tag{38}$$

in the expansion of η_g and ζ_g, see Eq. (25) [and having $\alpha \to 0$ for $T_g \to 0$ such as given by Eq. (29)] would yield hypoelasticity for vanishing shear rate. To see this, consider the stationary case of (24), $\dot{s}_g = 0$, implying $\gamma T_g^2 = \zeta_g v_{ii}^2 + \eta_g v^0_{ij} v^0_{ij}$. With Eq. (38), this results in a granular temperature that is quasi-linear in the shear rate for $\gamma_1 T_g \gg \gamma_0$,

$$T_g = \sqrt{(\zeta_1 v_{ii}^2 + \eta_1 v^0_{ij} v^0_{ij})/\gamma_1}, \tag{39}$$

and quadratically small for $\gamma_1 T_g \ll \gamma_0$,

$$T_g = (\zeta_1 v_{ii}^2 + \eta_1 v^0_{ij} v^0_{ij})/\gamma_0. \tag{40}$$

The ratio of volumetric and deviatoric granular viscosities is, for $\gamma_1 T_g \gg \gamma_0$, taken as

$$\zeta_g/\eta_g = \zeta_1/\eta_1 = 1/3, \tag{41}$$

implying

$$T_g = \bar{v}_s\sqrt{\eta_1/\gamma_1}, \tag{42}$$

with the intensity of stretching given as

$$\bar{v}_s \equiv \sqrt{v^0_{ij} v^0_{ij} + (\zeta_1/\eta_1) v_{kk}^2} \approx \sqrt{v^0_{ij} v^0_{ij} + v_{kk}^2/3}. \tag{43}$$

In conjunction with Eq. (28), the first limit, Eq. (39), leads to a rate-independent, hypoplastic regime, see Eq. (44). The second limit ensures that the relaxation rate in (28) is of second order, hence tiny, for very slow stretching. Neglecting it, the system becomes hypoelastic for $T_g \to 0$, sustaining stable granular structures and propagation of elastic waves. In addition, including only η_1, ζ_1 keep the results longer rate-independent, because they contribute to terms in the stress that are of second order in the strain rate, and hence negligible for the strain rates typical of soil mechanical experiments, while including η_0, ζ_0 would lead to contributions that are of first order, and more noticeable.

Retaining η_0, ζ_0 implies a return to hypoplastic behavior in the limit of $T_g \to 0$, with T_g given as $T_g^2 = (\zeta_0 v_{ii}^2 + \eta_0 v^0_{ij} v^0_{ij})/\gamma_0$, formally identical to Eq. (39) for $\eta_0 \gg \eta_1 T_g$, $\zeta_0 \gg \zeta_1 T_g$, $\gamma_0 \gg \gamma_1 T_g$. Taking $\zeta_0/\gamma_0 \ll \zeta_1/\gamma_1$ and $\eta_0/\gamma_0 \ll \eta_1/\gamma_1$, one can capture the observed, rather more elastic response to minute vibrations near $T_g = 0$, more below and in Sect. 3.3, where the attractors were possibly better reproduced with η_0, ζ_0.

3.2 Monotonous deformations

Starting at rest ($T_g = 0$) a granular 'element' may be deformed with *constant stretching* v_{ij}. It starts with any $\sigma_{ij} = \pi_{ij}$ and ρ in the range allowed for equilibria (Sect. 2.1).

Neglecting the quadratically small terms: $p_T \sim T_g^2$, $\eta_g v_{ij}^0 = \eta_1 T_g v_{ij}^0$, $\zeta_g v_{kk} = \zeta_1 T_g v_{kk} = (\eta_1/3) T_g v_{kk}$, and with $\alpha \approx 0$ by (29) for $T_g \to 0$, the initial stress rate is $\dot\sigma_{ij} = \dot\pi_{ij} = \mathcal{M}_{ijkl} v_{kl}$ by (31), (33) and (29) with (27) and (20), i.e. it is *hypoelastic*. Gradually, the granular temperature increases and saturates at the value given by Eq. (42).

Equation (42) is confirmed by the crackling noise of sheared thin layers, this increases with the rate of shearing and does not depend on the pressure. α increases up to α_h by (29) independently of $\bar v_s$ if this suffices for getting $T_h < T_g \ll T_b$. For $T_g \ll T_b$ the seismic and viscous terms are negligible in (31), then (32) and (27) yield, with (33) and $\dot\alpha = 0$ by (42),

$$\dot\sigma_{ij} = (1-\alpha_h)\dot\pi_{ij} = (1-\alpha_h)\mathcal{M}_{ijkl} \times \left[(1-\alpha_h) v_{kl} - \bar v_s \lambda \sqrt{\frac{\eta_1}{\gamma_1}} \left(u_{kl}^0 + \frac{\lambda_1}{\lambda} u_{\ell\ell}\delta_{kl} \right) \right]. \quad (44)$$

This relation is essentially *hypoplastic* (PSM): it is rate-independent, $\mathcal{M}_{ijkl}$ and u_{kl} are known functions of $\sigma_{ij} = (1-\alpha_h)\pi_{ij}$ by (31) and (32), the response polars by (44) are eccentric ellipses with two components in case of cylindrical symmetry and ellipsoids otherwise, see the articles by Kolymbas and Wu and Wu and Bauer in the book, *Modern Approaches to Plasticity* [33,34]. As for hypoplasticity the polars get bigger with more pressure $p = \sigma_{ii}/3$ and higher density, and are more eccentric with higher obliquity $\sqrt{\sigma_{ij}^0 \sigma_{ij}^0}/p$ [25]. They steer the stress path for constant stretching (i.e. proportional strain paths) towards a proportional one, thus the SOM-attractor (Sect. 1) is visibly attained. A promising quantitative agreement was achieved with the dimensionless factor

$$\lambda \sqrt{\eta_1/\gamma_1} \approx 10^2, \quad (45)$$

the parameters for the elastic energy named in Sect. 2.1, $\alpha_h = 0.8$ and $\lambda_1/\lambda = 0.1$ as indicated in Sect. 3.1. As hypoplastic relations have been amply validated for monotonous deformations (PSM) this is a support of GSH, which in turn provides a physical base for hypoplasticity.

A closer look reveals some differences. The rate-independence assumed for hypoplasticity does not hold by GSH for transitions, and is restricted to the temperature range $T_h < T_g \ll T_b$. During a transition by GSH for a new constant stretching the initial stress is swept out and a new stress path is determined by the new deformation, and the density is gradually changed except for isochoric deformations ($v_{ii} = 0$). Stress σ_{ij}, elastic stress π_{ij} and seismicity T_g are related by (31) throughout their evolution due to the imposed stretching. This resembles a SOM-transition in the observable response, but a gradual adaption of the hidden force-roughness to the observable stress (PSM) is not assumed in GSH. The increasing mechanical roughness is captured instead by the growth of the scalar and less hidden T_g.

Equation (44) may also be applied to uniform stretching with constant pressure $\sigma_{ii}/3$ and constant deviatoric stretching v_{ij}^0 which leads to $T_g > T_h$, this comes close to usual tests. With $\dot\sigma_{ii} = 0$ it yields the *dilatancy ratio*

$$v_{ii}/\bar v_s = f_d(\sigma_{ij}, \rho) \quad (46)$$

with a function f_d of stress and density which is determined by the elastic energy w_e. A modified f_d is obtained by keeping one pressure component constant, e.g. σ_3 in a triaxial test. Equation (46) engulfs ample experience with sand and is also obtained with hypoplasticity (PSM), it could be used to calibrate GSH-parameters appearing in (44). This is legitimate although v_{ij} is not precisely constant for constant pressure $\sigma_{ii}/3$ and deviatoric stretching v_{ij}^0 as the slight deviation of stretching v_{ij} does not matter for T_g by (42) and for $v_{ii}/\bar v_s$. This argument may be extended to other monotonous deformations with nearly constant v_{ij} so that many observations can be used for validation and calibration. A profound test still awaits GSH: steady state and shear banding. This is being worked out at the moment, and will be published soon.

Turning to monotonous deformations with *strong changes of stretching intensity* $\bar v_s$, we need further GSH-parameters and have to drop the rate-independence assumed with hypoplasticity. Hypoplasticity works empirically for $\bar v_s$ from about 10^{-6} to $10^{-3}\,\mathrm{s}^{-1}$. Combining (45) with the γ given in Sect. 3.1 leads to $\eta_1 \approx 10^{-2}\,\mathrm{Ns/(m^2K)}$ in (25). With it the viscous stress fraction by (30) is negligible so that (31) suffices in the indicated range of T_g. These estimates are crude, but may suffice for the time being. A rise of $\sqrt{\eta_1/\gamma_1}$ by a factor ϵ ($1 < \epsilon < 100$, say) would replace T_g and T_h by ϵT_g and ϵT_h from (24) and (29), and λ by λ/ϵ from (45). Thus the arbitrariness of ϵ does not matter for $\dot\sigma_{ij}$ with $T_g > T_h$ as long as p_T and $\eta_g \bar v_s$ are so small that (31) holds. A further calibration will be needed and possible if impeccable experiments with a wide range and jumps of $\bar v_s$ are available.

If a monotonous evolution in the hypoplastic regime is suddenly stopped the seismicity should decay within a time of at most $t_g \approx 10^{-3}\,\mathrm{s}$ (Sect. 3.1). This would cause creep or relaxation by (27) in the order of magnitude $\lambda T_g \Delta t_g < 10^{-6}$ with legitimate initial T_g and elastic compression Δ. This small amount suits to the experience with hard-grained samples that creep and relaxation do not arise after a sudden stop (except near state limits were the seismicity increases with unchanged boundary conditions). The stronger creep and relaxation observed with quartz sand by Matsuhita et al. [3] can be attributed to the grease between membranes and samples and to the servo-control (PSM). Tests with saturated undrained samples in a stiff device without grease could better confirm that changes from a stable state after a sudden stop are negligibly small.

If a monotonous deformation in the hypoplastic range is continued with the same deviatoric direction $v_{ij}^0/\bar v_s$, but a suddenly higher stretching intensity $\bar v_s$, the response by (44)

just after the jump of $\bar{v}_s$ is rather hypoelastic as the term with $(1-\alpha)$ dominates first, and gets hypoplastic by (32) after a transition. This was similarly observed in isobaric shear tests without membrane and grease by Tatsuoka et al. [35], such experiments could serve for the calibration of η_1 and γ_1.

One of us (G.G.) produced stationary shearing of a thin sand layer between rough plates with constant pressure and a shaken base. The applied T_g from about 10^5 to 10^7 K was nearly uniform as the diffusion factor χ exceeds by far the layer thickness (Sect. 2.2), and the contribution of shearing to T_g by (24) is rather uniform. The viscous part of stress by (30) with (25) can be substantial with the high T_g and $\bar{v}_s \approx 1\,\mathrm{s}^{-1}$, the entropic pressure p_T by (16) is no more negligible and the seismic energy by (17) is no more quadratic in T_g. Steady states could be captured with the generalization of (32) (Sect. 4.1) for validation and calibration. They could support (25) beyond the argument that (contrary to thermally activated viscosity) more seismicity causes more seismo-viscous resistance for a given $\bar{v}_s$.

3.3 Non-monotonous deformations

Deformations with *reversals* can occur in many variants, only a few cases are considered here to show that GSH is realistic also in that respect and that the parameters can be calibrated. We begin with isobaric cyclic shearing with small amplitudes, go over to bigger amplitudes and consider also seismically activated relaxation and creep. As before only orders of magnitude are given for a qualitative validation by means of attractors, and it is indicated how a more precise calibration could be achieved.

Usual *resonant column tests* produce isobaric cyclic shearing with pressure $p \approx 100\,\mathrm{kPa}$, frequency $f \approx 10^2/\mathrm{s}$ and shear amplitutes ψ_0 from about 10^{-7} to 10^{-4}. The observed response of sand is nearly rate-independent, about 1/100 to 1/10 of the pulsating part of the elastic energy is dissipated in one shear cycle, and the densification towards a lower bound e_d is faster for higher amplitudes [36]. The half-life of seismicity τ_g by (12) and (25) is $\tau_g \approx b\rho/\gamma_0$ for small T_g. About the same time is needed by (24) to attain a stationary T_g with a constant $\bar{v}_s$. With the proposed parameters the time τ_g is much shorter than the period $1/f$, thus the sand attains almost seismic rest with $T_g \approx 0$ periodically.

For sufficiently *small* amplitudes, T_g is small enough that $\eta_g \approx \eta_0$ and $\gamma \approx \gamma_0$. Assuming a uniform harmonic shearing $\psi = \psi_0 \sin(2\pi f t)$, the balance of seismic power (24) yields the biharmonic granular temperature

$$T_g \approx 2\pi f \psi_0 \sqrt{\eta_0/\gamma_0}\,[1+\cos(2\pi f t)]. \tag{47}$$

This is an interpolation between solutions of (24) near reversals and for extremal $\dot{\psi}$ with $\tau_g \ll 1/f$. The rates of elastic shearing ψ_e and volumetric strain Δ by (28) are thus rate-independent. The stress rate by (33) with (29) is $\dot{\sigma}_{ij} \approx \dot{\pi}_{ij}$ for small T_g. Thus its relation with stretching v_{ij} is also rate-independent by (47). A constant mean pressure, i.e. $\dot{\pi}_{ii} = 0$, leads to biharmonic rates of volume change v_{ii} as observed [36]. The assumed element dilates shortly before a reversal and contracts shortly afterwards. The observed damping ratios for small amplitudes could be reproduced with

$$\lambda\sqrt{\eta_0/\gamma_0} \approx 1, \tag{48}$$

but this is no more than a crude estimate. Quantifications could be obtained with numerical simulations, therein the rise of $\lambda\sqrt{\eta_g/\gamma}$ with growing T_g should be taken into account. Proper calibrations require tests with hollow cylindrical samples for better uniformity, and with observation of volume changes for different small amplitudes. The cumulative densification with constant pressure may serve to calibrate λ with suitably scaled T_g.

As in the hypoplastic range (Sect. 3.2) a rise of η_0/γ_0 by a factor ϵ, $(1 < \epsilon < 100$, say) would increase T_g and T_h to ϵT_g and ϵT_h and would reduce λ to λ/ϵ. Thus a rather arbitrary scaling of the granular temperature does not matter as long as rate-independence is justified.

The argument may be extended to small harmonic oscillations with anisotropic mean stresses in the stable range. With suitable $\sqrt{\eta_0/\gamma_0}$ the response is almost hypoelastic and the anleastic part is nearly rate-independent. Biharmonic fractions and non-linearity require again numerical simulations. Cumulative changes of shape (ratcheting) are obtaimed with GSH for anisotropic mean stresses. They could be observed with twisted hollow cylindrical samples under anisotropic mean stress, and used for calibration. Cylindrical samples of usual resonant column tests get gradually non-uniform so that evaluations get difficult (Sect. 4.3).

With bigger amplitudes T_g rises so that (47) and (48) are not even crude estimates. They would yield more than 10^3K for $\bar{v}_s > 10^{-3}/\mathrm{s}$, which is higher than in the hypoplastic range with $\bar{v}_s \le 10^{-5}/\mathrm{s}$. This overlap is less embarrassing by intuition than by theory. GSH yields again a nearly hypoelastic response in the vicinity of periodic minute intervals with T_g near 0. Pulsation between nearly hypoelastic and hypoplastic behavior, rate-independent nearly also in between. Otherwise T_g gets so big that $\eta_g \approx \eta_0$ and $\gamma \approx \gamma_0$ are no more justified, and the stress rate fraction by $\dot{\alpha}$ comes into play. This causes rate-dependence except for monotonous sections in the hypoplastic range. The uniformity of samples gets lost so markedly that a periodic response can no more be obtained. Therefore resonant column tests with big amplitudes (say $\psi_0 > 10^{-4}$) can hardly be controlled.

Youd [37] imposed *big shear cycles* with constant pressure p to drained saturated sand. A nearly p-independent low void ratio e was reached with different initial e by shear strains from ca. 10^{-3} to almost 10^{-1} with ca. 10 to 10^2 cycles per minute. The plot of e versus shear strain tended to a double loop with stronger contraction just after each reversal than

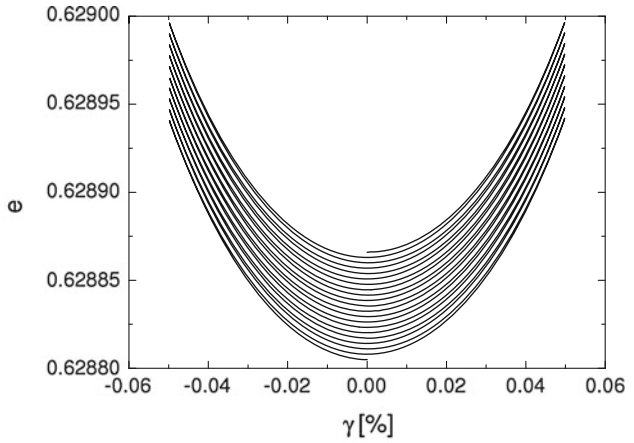

Fig. 1 GSH simulation of a triaxial version of Youd's experiments (see text), with the pressure kept constant, e denoting the void ratio, and $\gamma \equiv \varepsilon_{zz} - \varepsilon_{xx}$ the total shear strain. The *curves* are obtained taking the maximum and minimum void ratios as 0.875 and 0.58, $B_0 = 7\,\mathrm{GPa}$, $\gamma_0/b\rho = 25\,\mathrm{Hz}$, $\rho = 0.95\rho_d$ (implying a void ratio of $e = 0.63$), and the dimensionless parameters (see "Appendix") as $\sqrt{\zeta_1\gamma_1}/b\rho = 3.6\times10^4$, $\lambda_1/\lambda = 0.09$, $\lambda\sqrt{\eta_1/\gamma_1} = 114$, $\alpha = 0$, $(\gamma_0/\gamma_1)^2\, b_0\rho_d/B_0 = 2\times10^{-17}$, $\eta_1/\zeta_1 = 3$

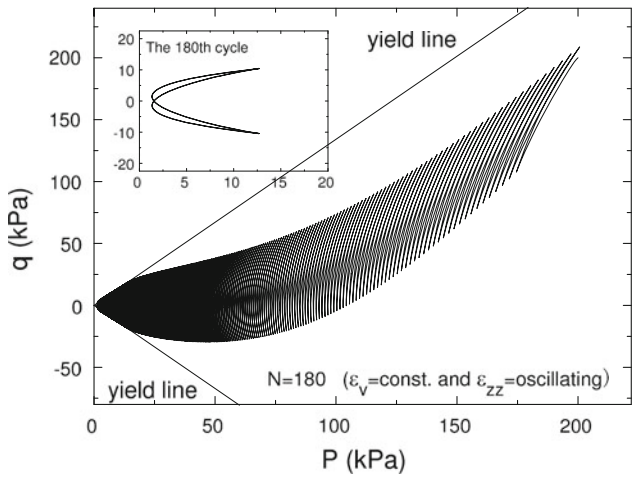

Fig. 2 GSH simulation of Wichtmann's experiment [38], depicting the relaxation of $q \equiv \sigma_{zz} - \sigma_{xx}$ and the pressure P in triaxial geometry, keeping the volume constant and the shear oscillating, $\varepsilon_{zz} = 3.8\times10^{-4}$, at $e = 0.663$. Inset amplifies the last calculated cycle. Parameters are the same as in Fig. 1

dilation just before, see Fig. 1. With the applied intensity of stretching $\bar{v}_s$ from ca. 10^{-4} to 10^{-2}/s the granular temperature T_g ranges from ca. 10^3 to 10^5 K by (42) with (45). It was nearly constant in each test as the changing volumetric strain matters little for T_g by (24) with (41), and as the resting intervals at reversals were much shorter than the shearing periods.

Youd's [37] experiments are impaired by repeated shear localizations with the applied big amplitudes (PSM). A better uniformity could be achieved in isobaric triaxial tests with smoolth endplates and so low axial deformation amplitudes that the stress obliquity remains subcritical. One can expect a densification up to lower average densities ρ for lower amplitudes, and an asymptotic double cycle of ρ (PSM). This is also obtained with GSH. Equation (27) with (19) and (42) indicate a more rapid cumulative densification for more intensive shearing, and with (31) for $\dot{\sigma}_{ii} = 0$ it reveals a stronger amount of contractancy $v_{ii}/\bar{v}_s$ after a reversal than of dilatancy before. An attractor near e_d with a double loop is also obtained by numerical simulations with GSH, this could serve to calibrate λ and ρ_d. Fig. 1 shows that a gradual densification is obtained with GSH as in Youd's tests, a saturation with a sufficient number of cycles and an asymptotic double cycle of void ratio versus shear strain is also reproduced. A quantitative agreement can be achieved with experiments which are underway, these will also enable to calibrate η_0 which matters only for small amplitudes near the attractor.

Wichtmann et al. [38] imposed *isochoric deformation cycles* to saturated sand in undrained triaxial tests. The implied zig-zag plot of strain vs. time means a constant stretching intensity $\bar{v}_s \approx 3.10^{-6}$/s (negligible resting intervals), i.e. $T_g \approx 3000\,\mathrm{K}$ by (42) with $\lambda = 10^{-6}/(\mathrm{sK})$. The observed zig-zag stress paths tend to a double cycle for high densities ρ or big amplitudes, and to a decay otherwise. A similar seismically activated relaxation up to a double stress cycle is obtained with (27) and (19) by numerical simulation (Fig. 2) and could serve to calibrate λ. As in the experiments the asymptotic state cycle (attractor) is only obtained with sufficient density and amplitude, otherwise the stress dwindles completely. Variations of stretching intensity $\bar{v}_s$ could reveal how far a rate-independent approximation is valid. The simulated asymptotic double stress cycle resembles observed ones for low void ratios, although these are distorted by the variable penetration of grains into the confining membrane (PSM).

Wichtmann's [39] triaxial tests with *small stress cycles* imposed to drained saturated sand enable a further validation and calibration. Jiang and Liu (to be published) simulated such evolutions with parameters from the present paper and reproduced Wichtmann's flow rule for cumulative deformations except near critical stress obliquities. The flow rule can be seen from (27) for constant mean stress, which yields a relation of stress ratios with stretching ratios for $T_g \propto \bar{v}_s$. The factor λT_g for the intensity of seismic creep and relaxation replaces an elaborate empirical factor in an accumulation model by Niemunis et al. [40]. Wichtmann's [41] results could be used to calibrate λ, $\sqrt{\eta_1/\gamma_1}$, and also $\sqrt{\eta_0/\gamma_0}$.

A closer look reveals some intricate points. Wichtmann's [41] flow rule holds even for overcritical stress obliquities, whereas these are taken to be unstable in GSH—though there is of course a characteristic time associated with the instability, and for time spans smaller this instability may persist also in GSH: GSH excludes already critical average

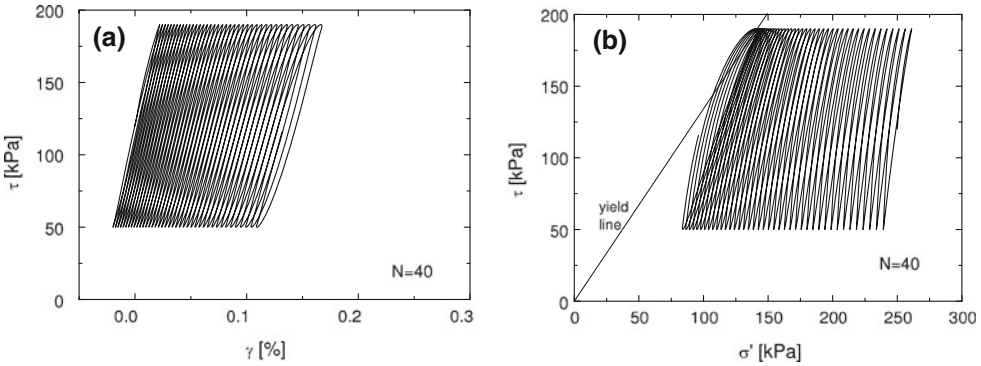

Fig. 3 GSH simulations of the Ibsen's experiments in triaxial geometry [42], with a constant volume, $e = 0.663$, and an oscillatory shear stress $\tau \equiv \sigma_{zz} - \sigma_{xx}$, while the pressure σ' relaxes and the shear strain $\gamma \equiv \varepsilon_{zz} - \varepsilon_{xx}$ grows. As observed the asymptotic stress cycle is a narrow lense which touches the yield line for steady states. Parameters are the same as in Fig. 1

obliquites, for which shear bands arise and disappear with the same rate. Asymptotic state cycles in the subcritical regime could not be attained by Wichtmann [41] and are not incorporated in Niemunis' et al. [40] theory. They are produced by simulations with GSH (Jiang and Liu, to be published) and are principally preferable for validation and calibration (PSM).

Stationary *ratcheting* was obtained e.g. (PSM) in undrained triaxial tests with deviatoric stress cycles by Ibsen [42]. He indicates without quantification that the asymptotic stress cycles are lenticular with at most critical obliquity, and that the mean pressure decreases or increases in the transition for initially medium or very dense samples, respectively. This is qualitatively reproduced by simulations with GSH (Fig. 3), which could provide a calibration of λ and the parameters for T_g. Other than in Wichtmann's [41] tests a flow rule for the average stress and rearrangement would require a kind of seismic pressure, but this should be rather rate-independent. As observed the asymptotic stress cycle is a narrow lense which touches the yield line for steady states. Further triaxial tests of this kind are underway and needed as the published ones yield at best qualitative attractors (PSM).

Recent constitutive models for sand with hidden state variables (PSM) are partly supported by GSH, and could thus be superseded. The assumed rate-independence is justified near states of rest and in the hypoplastic range, but cannot be defended for arbitrary reversals (cf. end of Sect. 3.2). Elastoplastic relations with back stress work with a narrow elastic range and different flow rules for deviatoric loading and unloading, whereas GSH produces an infinitesimal elastic range and anelastic flow nearby. Hypoplastic relations with intergranular strain imply an infinitesimal elastic range, and they reproduce the cumulative densification or relaxation as by GSH which is not achieved with recent elastoplastic models [43]. The hidden variables in both models may be related with a variable force-roughness, but their evolutions can hardly be judged and the energetics is not clear. Calibrations and validations are rather cryptic with both models, whereas calculations get more transparent with GSH, see "Appendix".

3.4 Collapse modes at the verge of stability

The elastic energy w_e of an element at the verge of stability is not changed by certain differential changes $\mathrm{d}u_{ij}$ and $\mathrm{d}\rho$ of elastic strain and density (Sect. 2.1). One can as well write $\dot{u}_{ij}$ and $\dot{\rho}$ for this eigenvector, but how can it be related with a *collapse mode* v^e_{ij} as for state limits? The volumetric part of v^e_{ij} is given by (34), i.e. $v^e_{ij} = -\dot{\rho}/\rho$. It differs from the elastic fraction u^e_{ii} in general. Starting at rest ($T_g = 0$),

$$\dot{u}^e_{ii} = v^e_{ii} - \lambda_1 T_g 3u_{ii} = -\dot{\rho}^e/\rho - \lambda_1 T_g 3u_{ii} \tag{49}$$

holds by (28) with $\alpha = 0$ from (29). The emerging T_g is thus proportional to the intensity of elastic stretching at a critical point. With $u_{ii} = -\Delta$, (27) and (49), the collapse mode is related with the eigenvector by

$$v^e_{ij} = \dot{u}^e_{ij} + \frac{1}{3}(\dot{\rho}^e/\rho + \dot{u}^e_{ii})\left(\frac{\lambda}{\lambda_1 \Delta} u^0_{ij} - \delta_{ij}\right). \tag{50}$$

It is rate-independent and could be normalized with the intensity $\bar{v}^e_s$ by (43), this correspondends to observed modes for state limits (PSM). A rearrangement along an eigenmode at the verge of convexity means that the elastic energy w_e is differentially indifferent, i.e. $\dot{w}_e = 0$ for the indicated v^e_{ij} and $\dot{\rho}^e/\rho$. Thus the mechanical power imposed to an RSE is maximally transformed into seismicity, whereas w_e increases for other differentials of elastic strain and density.

Consider for illustration a cylindrical sample with a dead load. Equation (50) can be written with principal components, dead load means $\dot{\sigma}_1/\sigma_1 = -v^e_2$. The element may have constant radial pressure or volume. A state at the verge of stability may be attained by axial shortening with smooth plates. Switching then to dead load causes a spontaneous growth of seismicity. The cylinder gets shorter and wider up to a new shape and state of rest with the given dead load. Such a *chain reaction* may be considered as a succession of eigenvalue problems as long as the RSE is at the verge of convexity. Observed states and rates of shape and state at the verge of stability could be compared with calculated ones.

A precise validation and calibration gets difficult as the verge of stability cannot be attained with uniform stretch-

ing, and as the representation of w_e by (5) does not suffice (Sect. 2.1). Real samples exhibit chain reactions including localized shearing with dilation or contraction. Uniform state limits may at best be assumed for spatial averages, experiments reveal localizations for overcritical stress obliquities (PSM). Bifurcations with new (presumably polar) degrees of freedom for localized granular phase transitions are left aside for the moment, it is not yet clear whether these are necessary.

4 Non-uniform-evolutions

4.1 Evolution equations, initial and boundary conditions

In general the *granular entropy production* is given in GSH by

$$T_g[\partial_t s_g + \nabla_i(s_g v_i)] = R_g = -\gamma T_g^2 + \zeta_g v_{ll}^2 + \eta_g v_{ij}^0 v_{ij}. \tag{51}$$

With the term $\nabla_i(s_g v_i)$ from the smoothed velocity v_i the left-hand side is $T_g \dot{s}_g$ for a convected 'element'. Aside from the term $-\gamma T_g^2$, the right-hand side is positive definite as required by the Second Law of thermodynamics (Sect. 4.2). The factor T_g and the viscous terms (with $v_{ij} = (\nabla_i v_j + \nabla_j v_i)/2$) are the same as in (24), the viscosities depend on T_g by (25).

The general *thermal entropy production* in GSH is more complex, viz.

$$T[\partial_t s + \nabla_i(s v_i - \kappa \nabla_i T)] = R \equiv \gamma T_g^2 + \kappa(\nabla_i T)^2 + \beta^\rho(\nabla_j \bar{\pi}_{ij})^2 + \beta \pi_{ij}^0 \pi_{ij}^0 + \beta_1 \pi_{ll}^2 \tag{52}$$

for hard grains with negligible thermally activated viscosity. The left-hand term $\kappa \nabla_i^2 T_g$ in (52) with the thermal diffusion factor κ in addition to $\dot{s}$ corresponds to the term $\chi^2 \nabla_i^2 T_g$, it is a source of entropy off equilibrium. The term γT_g^2 is the same with opposite sign as in (51) for the balance of energy. The term $\kappa(\nabla_i T)^2$ is a further source of entropy as $\nabla_i T = 0$ holds at a thermodynamic equilibrium. The terms with $\nabla_i T$ remain for seismodynamic equilibria and serve then to calculate the field of T from the one of T_g by (51). The term with

$$\bar{\pi}_{ij} \equiv \pi_{ij} - \rho g_i r_j, \tag{53}$$

the vector of gravity g_i and the position vector r_i, contribute to the entropy production as $\nabla_i \bar{\pi}_{ij}$ vanishes by (55) at a thermodynamic equilibrium. Factor T and the further right-hand terms in (52) are the same as in (18). This is thus properly extended as it is positive definite in all deviations form thermodynamic and seismodynamic equilibria.

The general evolution equation for the *elastic strain* reads

$$\dot{u}_{ij} \equiv \partial_t u_{ij} + \nabla_i(u_{jk} v_k) = (1-\alpha) v_{ij} - \frac{u_{ij}}{\tau} - \frac{u_{ll}\delta_{ij}}{\tau_1} - \beta^\rho \nabla_k \frac{(\nabla_i \pi_{jk} + \nabla_j \pi_{ik})}{2}. \tag{54}$$

Except for the convective term this agrees with (27) and may be substituted with (19). The further term with a relaxation factor β^p accounts for dissipative forces to eliminate $\nabla_k \pi_{ik}$—quite analogously as $\nabla_k T$ is eliminated. It is a 'force' for the entropy production by (52) with (53), with its two parts it preserves the symmetry of the tensor u_{ij}.

The *total stress tensor* in GSH is generally given as

$$\sigma_{ij} = p_T \delta_{ij} + (1-\alpha)\pi_{ij} - \eta_g v_{ij}^0 - \zeta_g v_{ll}\delta_{ij} - \rho g_i r_j \tag{55}$$

for hard grains. The evolution equations are completed by the conservation equations for mass

$$\partial \rho / \partial t + \nabla_i(\rho v_i) = 0 \tag{56}$$

and linear momentum,

$$\rho(g_j + \partial v_j/\partial t + \nabla_j v_l^2) = \nabla_i \sigma_{ij} \tag{57}$$

with gravitational acceleration g_i. The Eqs. (51), (52), (54) and (55) are the only legitimate ones of first order in the elastic strain within the hydrodynamic theory, extended by granular temperature and entropy. Transitions to equilibria and deviations from it are properly captured (Sect. 4.2).

The representations for the elastic and kinetic energies need not be the ones by (5) and (10) with density-dependent factors B and b, but they must satisfy general requirements. The Onsager matrix for the relation of "forces" and "flows" may have more than the one off-diagonal coefficient α. Further off-diagonal coefficients need to be introduced as necessitated by experimental data, rendering the granular hydrodynamic theory more intricate, see "Appendix".

Boundary conditions are needed in addition to the ones for equilibria (Sect. 2). Usual thermostats may suffice, seismostats for T_g have to be clarified (Sects. 2.2, 2.3 and 4.5). Pressure-free boundaries should be avoided because of decay (PSM), boundary pressures can be imposed via a membrane or mat. Adjacent deformable solids can be elastic and can move alongside with the granular body, but not in general. The granulate can move together with a solid at a rough surface, but can also slip or get separated. Boundaries with moving solids can be intricate, only a few simple cases will be considered in the sequel.

Initial conditions for the field variables will usually be specified for a state of rest (i.e. $v_i = 0$ and $T_g = 0$). The density field (or e instead of ρ) has to be estimated from the kind of placement or from probing. The stress field $\sigma_{ij} = \pi_{ij}$ at rest may be determined by $\nabla_j \sigma_{ij} = \rho g_i$, and is (as the density ρ) severely confined by stability (Sect. 2.1). Assuming a straight previous elastic strain path and rigid boundaries without or with activated friction is a legitimate approach to

π_{ij} if an initial ρ field is given [24]. Attractors in the large (Sect. 4.3) may instead be employed if the past is adequately known (Sect. 4.3). This can lead to π_{ij} and also ρ in case of past seismicity. Otherwise the initial state remains rather indeterminate, and thus also the onset of subsequent evolutions (PSM).

4.2 The total energy

Consider a granular body with adjacent rigid or elastic bodies. The interfaces are rough or smooth so that grains are fixed or can slide along solids. Shear localization and decay may be excluded for simplicity, particularly along interfaces and free surfaces. The *total energy* is

$$E = E_g + E_e + E_k + E_t \tag{58}$$

with gravitational, elastic, kinetic and thermal parts. The latter may frequently be ignored, especially if T is kept constant. With specific energies per unit of volume E can be expressed by the integral

$$E = \int (w_g + w_e + w_k + w_t)\, dV \tag{59}$$

over the volume V of connected granular and solid bodies. Movable boundaries with fluids require additional surface integrals, e.g. along a confining membrane with pressure from a reservoir. The specific gravitational energy w_g of quartz sand changes by roughly 20 J/m^3 for a change of height by 1 mm. The specific elastic energy w_e of sand has the same order of magnitude for 100 kPa mean pressure (Sect. 2.1), i.e. ca. 10 m below a free surface. The heat-like seismic energy w_s is roughly 10^{-3} J/m^3 for $T_g = 10^6$ K with the b_0 given in Sect. 2.2, and is thus negligible for E in the hypoplastic regime—let alone the hypoelastic one. The kinetic energy $\rho v_i v_i/2$ from the average velocity v_i may also be neglected for slow evolutions to which we focus in the sequel.

The *stablility* should be judged by means of E for stationary boundary conditions. These imply adjacent solids which can be movable and may be shaken (seismostats), and movable granular surfaces. The balance of linear momentum can be substituted by the principle of virtual work, but this does not mean an extremum of E in general. Only equilibria with stationary position and state have $\delta E = 0$, i.e. E is differentially stationary for variations of position and state. Stable equilibria require $\delta^2 E > 0$, unstable ones have $\delta^2 E < 0$, and $\delta^2 E = 0$ holds at the verge of stability for certain variations of position and state.

The functional dependence of the energy E on the state field (u_{ij}, ρ) and its change during a collapse is not sufficiently determinate in general. It is not yet clear when and how eigenvector fields (modes) for neighboured static equilibria could be calculated with GSH. Collapse does not mean a kinematic chain (collapse mode) in general with limit stress states as often assumed (PSM), but a *chain reaction* by a succession of modes. This could mean that the rate-dependence as for elements near $T_g = 0$ (Sect. 3.4) is not justified in general. As this problem is not yet solved, we focus on *seismically activated stabilizations*, i.e. quasi-static evolutions with slowing-down redistributions of position and state which are driven by stationary shaking and gravity. This means $\mathrm{d}E/\mathrm{d}t < 0$ with $\mathrm{d}^2E/\mathrm{d}t^2 > 0$ and requires suitably specified seismostats. The shaking of adjacent solids may be harmonic or intermittent and should produce a stationary field of period-averaged seismicity $\bar{T}_g$. Stabilizations tend to a stationary energy, but this asymptote (which is not a seismodynamic equilibrium) need not be attained in applications. A stabilization may be called *self-healing* if a desired configuration and state is regained after a damaging action.

Let us see by means of examples how this could work with GSH. Consider first an *elastic pile* which is clamped at the bottom and surrounded by a sand layer. At the beginning the pile may be upright and the sand dense. The energy without seismic and thermal parts, i.e.

$$E = E_{g1} + E_{g2} + E_{e1} + E_{e2} \tag{60}$$

for pile (1) and sand (2), increases by pushing the pile head and decreases partly by its release. A part of the imposed mechanical work is regained by unloading, a major part is dissipated by loading and less by unloading. The remaining part is elastic (E_{e1} and E_{e2} grow) by jamming of the unloaded pile and the sand nearby, plus gravitational by tilting of the pile with head structure and by lifting of dilated sand (reduction of E_{g1}, rise of E_{g2}). One could calculate E with elasticity for pile and GSH (or an equivalent) for sand, but this is not needed to judge the potential of self-healing. Shaking of bottom or pile head causes relaxation of pile and sand plus settling of sand by densification. E returns to the previous minimum with upright pile and dense sand, and remains there with continued shaking.

Not quite, however, as a closer look reveals. Shaking with stationary, but inevitably non-uniform T_g would lead to a seismodynamic equilibrium with complete relaxation, hydrostatic pressure and almost maximal density (Sect. 2.2). This would take such a long time that it could not really occur. A shaking base would excite sand and pile via hysteretically damped waves. The bigger amplitudes near the pile and the free surface prevent a complete relaxation and densification. Shaking the pile head can excite the neighboured sand only as far as seismic waves are generated in the interface of pile and sand and are propagated. A strongly distorted and very flexible pile could not return by shaking its head, and the sand nearby would be strongly dilated and contracted with a rather low average density.

Such evolutions could principally be simulated with GSH, but the numerical expenditure would be enormous and inadequate. In spite of an initial indeterminacy one may state that

a pile in sand is capable of self-healing if it is stiff enough and its foot is clamped. A mat upon the sand surface should prevent skeleton decay and reduce the amplitudes (PSM). If a solid layer is not available to fix the pile foot this should be so deep that it is not bent. This could be assessed with GSH (or a substitute) for a new strong loading after self-healing.

Consider now a *rigid tower* with a shallow foundation upon sand. With high density a minute tilt $\delta\psi$ from the upright position changes the energy by

$$\delta^2 E = \left(-m_g h_g + c_1 B \left(\frac{mg}{Bb^2}\right)^{1/3} b^3\right) (\delta\psi)^2 \tag{61}$$

with tower mass m, centre of gravity height h_g and foundation width b. The hypoelastic stiffness is proportional to B and to $(p_b/b)^{1/3}$ by (3) and (32) with base pressure $p_b \propto mg/b^2$. The factor c_1 is determined by the base shape and the pressure distribution below, which could be estimated with Jiang and Liu's [22,23] Granular Elasticity. The tower is at the verge of stability for $\delta^2 F = 0$ and would topple in a chain reaction.

A lower h_g/b is necessary for self-healing from a tilted position with lifted sand by dilation nearby. The tower would topple if E is at the verge of convexity, but $\delta^2 E$ can no more be calculated as by (61). The pressure and density distribution under a tilted tower could no more be estimated as the GSH-equations get ill-posed for neighboured static equilibria. The mode for $\delta^2 E = 0$ is not hypoelastic as it implies an anelastic densification and an average base settlement.

A more feasible approach requires a slenderness and tilt well below the verge of stability. A safe tilt could be estimated with GSH (or an equivalent) for a temporary design load. This leaves back a skew near-field of stress and reduced density. Subsequent calculations could be carried out with small horizontal load cycles $\pm\Delta H$. If the tower turns back for any height and direction of ΔH self-healing may be expected. A few test cycles would indicate how the tower returns and how dilated sand is densified. This was done by Sturm [44] with hypoplastic and elastoplastic relations and was validated by model tests.

A more elegant approach could be achieved with an average stationary filed of granular temperature $\bar{T}_g$ by continued shaking with small amplitudes. In the stable range the response is nearly hypoelastic (Sect. 3.3). With a hysteretic energy loss of about 1/100 per cycle the geometric damping by radiation of elastic waves dominates for wavelengths above ca. $b/10$. The stress- and pressure-dependent stiffness may be substituted by an average modulus and a Poisson ratio ca. 1/3, i.e. a constant velocity c_s of transversal waves. The amplitudes of harmonically excited blocks on an elastic half-space can be calculated by means of substitute stiffness and damping factors, which depend on frequency f, for wavelengths $c_s/f < b/2$ [45].

The imposed power is radiated off in proportion to the kinetic energy of the block. Period averages of stretching intensities can be estimated by $\bar{v}_s \approx f\bar{V}_s/c_s$ with resultant velocities $\bar{V}_s$. These can be obtained for the block as indicated, and can be estimated for the near-field from the balance of power by assuming its spatial distribution. Small amplitudes yield $\bar{T}_g \approx \bar{v}_s\sqrt{\eta_0/\gamma_0}$ by (47). This determines the average elastic strain rate $\dot{\bar{u}}_{ij}$ by (27) with the average stretching $\bar{v}_{ij}$, and the average stress rate $\dot{\bar{\sigma}}_{ij}$ by (31) and (44).

If the $\bar{T}_g$-field is thus given in sufficient detail one can calculate the field of average stretching $\bar{v}_{ij}$ and and stress rate $\dot{\bar{\sigma}}_{ij}$ by means of the balance of momentum. Estimates may suffice instead as the input data are rarely precise. Zones with negligible average stretching ($\bar{v}_{ij} = 0$) experience *seismic relaxation* with an alignment by the average stress via $\bar{u}_{ij}$ and (3), and an intensity

$$|\,\dot{u}_{ij}\,| \approx |\,u_{ij}\,|\,\lambda\bar{T}_g. \tag{62}$$

Zones with negligible relaxation experience *seismic creep* with an alignment by $\bar{u}_{ij}$ and an intensity

$$|\,v_{ij}\,| \approx 2\Delta\lambda\bar{T}_g, \tag{63}$$

wherein $|\,u_{ij}\,| \approx 2\Delta$ is assumed for simplicity. As outlined in Sect. 3.3 λT_g is not changed by rescaling T_g via $\sqrt{\eta_0/\gamma_0}$, this eases the calibration. Typically λT_g ranges from about 10^{-8}/s to 10^{-5}/s for small amplitudes.

The field of density and stress is skew after a temporary horizontal loading and could turn back the tower slightly. Its relaxation by 1/10 (say) needs a time $\tau_r \approx 0.1/\lambda\bar{T}_g$. With a suitable stress alignment a tilt of 10^{-2} (say) is returned by seismic creep in a time $\tau_c \approx 10^{-2}/\Delta\lambda\bar{T}_g$. With $\Delta \approx 10^{-3}$ this means $\tau_c/\tau_r \approx 10^2$, i.e. self-healing occurs mainly by creep as the relaxation ends much earlier. So the tower could be pushed back by skew pressures at best at the beginning, but how can it return further on?

Sturm [44] showed with hypoplastic relations that sand under the risen side of a foundation is more dilated than under the lowered side, and settles more by average-free cyclc loading at the higher side so that the tilt is reduced. The sand is almost equally distorted on both sides by a forced tilt, but less dilated with increasing pressure on the former leeward side than with decreasing pressure on the windward side. The energy drops faster with a back-tilt as thus the sand loses gravitational energy more rapidly. The rise of the centre of gravity by back-tilt is more than compensated by an average settlement, which goes on after the tower is upright and the sand is re-densified. This is confirmed by model tests and calculations [44].

The proposed method could also be applied to other foundations, but with less precision. The $\bar{T}_g$-field around a pile by a head excitation may be estimated by means of elastic waves, but this is debatable with the bigger amplitudes near the pile. A floating pile which was tilted down to its foot cannot turn back as E can be the same for different tilts. A group

of piles cannot turn back and can even rise by strong head shaking with a permanent moment until the whole structure collapses.

A single pile can move past sand with *axial symmetry*. With high density and monotonous shift the resistance at the shaft rises strongly as the sand is jammed by confined dilation. Rebstock [46] could reproduce observed resistances with hypoplasticity, but not the strong unjamming by further shifting. The latter can be attributed to a dramatic rise of T_g by localized shearing, this is not in the present reach of GSH. The sand is relaxed by periodic shaking of the pile head, this could be estimated by (62) with $\bar{T}_g$ from elastic waves via (24). The pile creeps with increasing rates under an axial dead load. An estimate by (62) gets debatable near the verge of stability as then waves can no more be propagated.

4.3 Attractors in the large

The observed asymptotic response of sand bodies with suitable boundary conditions can be used for validation and calibration of calculation models (PSM). Such *attractors in the large* will be discussed here with GSH. They can also help to understand limitations and to specify boundary conditions, in particular with shaking.

SOM-fields (swept-out memory) can be obrained with monotonous displacements of soil bodies past sand, and also by filling and excavation as long as localized shearing and collapse are avoided. This was observed e.g. with a concrete block by pushing it into sand with a skew guided jack (PSM). Apart from an irregular onset due to indeterminate details of installation one could thus validate and calibrate GSH beyond element tests. Spatial fluctuations of stress and void ratio are partly ironed out by monotonous deformations, this gain of symmetry could also be obtained with GSH in the stable range.

The symmetry can get lost if the verge of stability is reached and the boundary conditions prevent a stabilization (Sect. 4.2). A block with a dead load can topple suddenly, whereas sand near a penetrating guided pile can be homogenized by approaching state limits in the near-field. Moving a wall past sand leads to shear bands and earth pressures which deviate from Coulomb's assumptions. Such *critical phenomena* with a sudden drop of energy and spontaneaus new degrees of freedom are beyond the present reach of GSH.

Periodic state fields can be attained by slow cyclic displacements of solid bodies past sand, and also with superimposed monotonous shift (ratcheting). For instance, a pile in sand can wake an asymptotically cyclic reaction by shifting it repeatedly up and down, and also with additional monotonous shifting. Pressure and void ratio in the near-field can get periodic, their averages are determined by the amplitudes and the far-field. Periodic fields can also be generated with torsion, tumbling or driving (PSM). The attained symmetry gets lost by critical phenomena in case of too big amplitudes or insufficient guiding.

The back-analysis of evolutions up to periodic fields gets cumbersome or impossible with elastoplastic or hypoplastic relations as the equations are rather obscure, in particular with hidden variables needed for reversals. The GSH-equations remain transparent although a spatio-temporal *intermittent seismicity* cannot easily be captured. The often assumed rate-independence could be checked and superseded by means of periodic attractors. It is justified for the hypoplastic range and as far as the duration of waiting intervals does not matter. Rate-dependence arises near reversals due to drastic changes of streching, its observation can be of use for calibration (Sects. 3.2 and 3.3). Initial fluctuations are ironed out by intermittent seismicity in the stable range. Critical phenomena are left aside as strange attractors are not yet at hand.

The approach with nearly hypoelastic relations proposed in Sect. 4.2 could also work with attractors in the large. The stretching of samples in usual *resonant column tests*, e.g., is not spatially uniform. A seismically approached periodic density field may be assumed (Sect. 3.3), but a closer look reveals defaults. A stationary non-uniform period-average $\bar{T}_g$ would mean an average rate of densification by (63), this would require $\lambda = 0$ for a stationary average density. Like the amplitude $\bar{T}_g$ should be proportional to the distance r, this requires an excess of axial pressure near the axis so that the sample can get shorter by seismic creep, which in turn excludes $T_g = 0$ for $r = 0$. A back-analysis of observed attactors will therefore be difficult.

Resonant column tests with shearing amplitudes above ca. 10^{-4} do not lead to a periodic response as samples lose the cylindrical shape. One may doubt a periodic attractor also with smaller amplitudes as a visible loss of shape could take more time than spent unsually. Therefore estimates like (62) and (63) cannot easily be improved. This holds also true with anisotropic average stresses: the sample creeps indefinitely and loses its cycindrical shape so that a periodic response cannot strictly occur.

Consider now the *propagation of plane waves* by GSH in a dry sand layer from a solid base. Without inclination and with small amplitudes T_g gets nearly biharmonic as by (47), and reduces the amplitude off the base by seismic damping. The stationary vertical pressure by weight causes biharminic oscillations of density. The amplitude grows near a free surface so that T_g is no more biharmonic. The layer is densified by repeated propagations if it is not dense from the very beginning. If the layer has a subcritical inclination it moves downwards by each propagation.

An attractor in the large can be attained by stationary shaking of the base. With small amplitudes the average density $\bar{\rho}$ comes close to the upper bound ρ_d near the base. The average horizontal pressure gets stationary by relaxation with

few propagations, the stress cycles get symmetric. A zone with periodic changes is approached earlier near the base, the lower T_g further above due to damping causes a slower approach. With a subcritical inclination the layer tends to a kind of stationary ratcheting with asymmetric stress cycles.

With bigger amplitudes T_g is no more biharmonic and reduces the amplitudes more markedly off the base. With strong shaking the kinetic energy from the base can no more be propagated by waves as the sand loses its average elastic energy by relaxation. Then the seismicity is only spread by diffusion with small half-value lengths (Sect. 2.2). Needles to explain that simulations get harder with bigger amplitudes, and as yet impossible beyond the verge of stability due to localizations.

Further attractors with small amplitudes can be related with the examples in Sect. 4.2. The self-healing of a *clamped pile* in sand can occur by exciting its head horizontally. If its oscillation amplitude u_0 is lower than ca. 10^{-5} times its diameter d the $\bar{T}_g$-field may be estimated via the propagation of elastic waves. An attractor is approached with the pace $\lambda \bar{T}_g$ by (62) and (63). One could observe with higher frequencies f how far the pace is proportional to $u_0 f$ as by GSH for low T_g.

An asymptotically periodic response could be exploited with more expenditure. The overall compliance and damping of the sand could more easily be observed than the distribution of bending and densities. The latter could be calculated iteratively with GSH for validation and calibration. This would also work with a weakly tumbling pile head. Bigger amplitudes could cause so high T_g that the sand gets totally unjammed near the pile and cannot propagate waves. The observed sinking of turbine foundations into dense sand by a few cm per year (V. Ilyichev, personal communication) could serve for calibration.

A *tower with a shallow foundation* and low enough centre of gravity could turn back and redensify neighboured sand by means of a symmetric head excitation, during and after this self-healing its sinks further on. The pace decreases as a growing part of the imposed kinetic energy is absorbed by the increasingly embedded flanks of the foundation, and due to on-going densification below if the sand was not dense before. The observed amplitude-dependent pace could be used for calibration. The repeated return of a TV tower in Moscow with a ring foundation on dense sand (B. Mazurkiewicz, personal communication) could serve for calibration.

A *pile with guided foot* and a vibrator on top can produce axi-symmetric attractors in surrounding sand (PSM). Without average shift the state cycle field for small amplitudes could be simulated by means of almost hypoealstic waves, this could help to validate GSH near $T_g = 0$. With a stationary average shift and small amplitudes shear waves cannot likewise be propagated, simulations could then help to understand the verge of convexity. A kind of granular flow could also be generated with bigger amplitudes, but then critical phenomena could impede calculations.

Torsion tests with vibrators enable further periodic attractors (PSM). A loss of symmetry can be avoided with guided twisted solids at sand and control of average pressure $\bar{p}$ or density $\bar{\rho}$. Without average shift the asymptotic $\bar{\rho}$ or $\bar{p}$ is determined by the controlled $\bar{p}$ or $\bar{\rho}$, respectively, and by the amplitude ψ_0 and frequency f. An annular thin layer between rough horizontal and smooth vertical rings could get so uniform that that it may be considered as an element. Vibrations from above or below could generate a uniform time-averaged seismicity. Steady states with stationary shift and weak shaking could similarly be evaluated; $\bar{T}_g$ gets higher by average shearing, but could be low enough for neglecting the viscous resistance and the dynamic pressure.

Periodic fields with radially and axially decreasing seismicity could be obtained with twisted and shaken axisymmetric solids in sand. Without average torsion and with small amplitudes the field of $\bar{T}_g - T$ could be estimated by means of hypoelastic waves. Simulations with GSH could show how far this works, this could likewise be tried with ratcheting. Stationary fields could also be obtained with stronger shaking as long as deterministic chaos beyond the verge of stability is avoided.

Continuously vibrating solids may be named *seismostats* if they generate stationary $\bar{T}_g$-fields in adjacent granular bodies. Other than with thermostats a net input of seismic power is needed for the loss into heat. The seismic energy is spread by diffusion in case of seismodynamic equilibria, and by hypoelastic waves in the differential vicinity of thermodynamic equilibria. For cases in between the GSH-equations are non-linear so that numerical iterations are needed even for layers with gradients only along the normal. Simplified equations like (1) for estimating T_g-fields could thus be improved. Some field observations during earthquakes (PSM) could serve for validation and calibration.

5 Conclusions and outlook

5.1 What has been achieved

The present paper provides arguments for the validity of GSH and proposes some improvements and quantifications. The verge of stable equilibria seems to agree with state limits, both cannot be attained with uniform deformations. Seismodynamic equilibria are scaled by means of granular boiling with an estimated $T_g \approx 10^9$ K for dry fine sand. This suffices for the mainly considered slow evolutions with granular temperatures T_g below ca. 10^6 K, although seismometers for measuring T_g are not yet available. The seismic energy $w_s \propto T_g^2$ matters more than the thermal one w_t in spite of

$w_s \ll w_t$ as only grain contacts are affected by w_s during its transition into heat.

A thought electromagnetic excitation helps to understand that the transferred stress is proportional to the elastic one, can be smaller and dwindles in case of constant T_g. Only few parameters are needed for the hypoplastic range with monotonous isotachic deformations. The observed rate-dependence just after a sudden rise of stretching intensity $\bar{v}_s$ suits to GSH, but could not yet be quantified. The known crackling noise supports $T_g \propto \bar{v}_s$ independently of pressure p for constant $\bar{v}_s$.

The rate-independent small hysteretic damping ratio in resonant column tests suits to GSH for small T_g, this supports the proposed granular viscosity η_0 for $T_g = 0$ and explains the observed almost hypoelastic behaviour near states of rest. The rate-dependence for bigger amplitudes by GSH cannot be quantified by such tests as then the samples lose their cylindrical shape. Isochoric cyclic deformations cause a gradual relaxation in triaxial tests, its reproduction by GSH can be used for calibration. The densification up to double cycles of void ratio, observed with isobaric cyclic shearing and different amplitudes, can likewise be reproduced, and also asymptotic stress cycles by isochoric ratcheting. For all these evolutions the remaining arbitrariness of scaling T_g does not matter as long as deviations from rate-independence are minor.

The equations for elastic strain u_{ij} and T_g are the same for non-uniform evolutions except for convection terms as other terms with gradients are negligible in the considered range. Stabilizations can be judged by means of the total energy which gets minimal by stationary shaking. This is shown for clamped piles and towers on shallow foundations, both can turn back with re-densification from a tilt with dilation. The progress of seismic creep and relaxation can be estimated with an average T_g from elastic waves. Limitations of this approach could be explored by axi-symmetric model tests.

Evolutions by GSH can be judged by means of attractors in the large. Hypoplastic state fields attained in experiments strengthen GSH as far as localized shearing and collapse are avoided. Periodic state fields can be attained by slow cyclic displacements and ratcheting of solids past sand in the stable range. Such attractors can more reliably be reproduced than with elastoplastic or hypoplastic relations, the GSH-equations are also more transparent and robust. GSH can supersede high-cycle accumulation models which cannot reproduce observed attractors. Localized shearing and collapse have as yet to be left aside.

5.2 What could be further done

The *energy functions* in GSH should be improved. The specific elastic energy w_e should depend on the third invariant of elastic strain. A more elegant representation of w_e for low densities and stress obliquities is desirable. It will be more difficult to introduce polar quantities for shear bands. They arise along rough boundaries by shearing of thin layers, and spontaneously inside with an overcritical average stress obliquity (PSM). Thin layer shear tests with shaking base could help to improve and quantify the seismic energy w_s and the granular viscosity for high T_g and $\bar{v}_s$.

The extension for *pore water* will not be difficult with full saturation. For equilibria the energies with given u_{ij} and T_g are hardly reduced by the lower granular surface energy, but the factor γ for the relaxation of s_g (and T_g) by (12) is bigger by the viscous resistance of water between the grains, more so if these are small. Water matters little for the quantities α_h, λ/λ_1, ζ_g/η_g and $\lambda\sqrt{\eta_1/\gamma_1}$ which count in the hypoplastic regime. Wichtmann [41] observed the same cumulative effects for small amplitudes without and with water, this seems thus to have no influence also on $\lambda\sqrt{\eta_0/\gamma_0}$. It is rather evident that the granular viscosity η_g increases likewise with water as the relaxation factor γ, so the quantities named above should only depend on grain properties. Pore water causes an additional viscosity η which appears already in GSH, but resonant column tests indicate that η is negligible. As known in soil mechanics the water pressure increases the total pressure by $p = p_g + p_w$, and deviations of p_w from hydrostatic values cause seepage independently of T_g.

The *calibration* of parameters beyond the hypoplastic range could proceed as indicated in Sects. 3.2 and 3.3. $\lambda\sqrt{\eta_0/\gamma_0}$ could be determined with minute oscillations, λ and λ_1 could be calibrated with isochoric deformation cycles and ratcheting. A better scaling of T_g and T_g-dependent parameters could be obtained from tests with variation of the stretching intensity $\bar{v}_s$ over more than three decades. Rapid shearing of thin layers with strong shaking ($\bar{v}_s \approx 1$/s and $T_g \approx 10^7$ K, say) could help to calibrate b_o and η_1.

Matching attempts could reveal the need for *further parameters*. Those for the elastic energy should better capture the verge of stability, and beyond it localizations will presumably require polar quantities. A further transfer factor α_1 could be introduced if the calibration of λ and λ_1 does not suffice. Asymptotic state cycles with small amplitudes should be thoroughly investigated before introducing further parameters. One should not expect, however, a precise matching with few parameters for several decades of T_g.

Model and field tests can help to specify *initial and boundary conditions* in the stable range. Simplified average T_g-fields will be needed to estimate the alignment and progress of stabilizations, therein the balance of seismic energy and the preference of maximal dissipation could be of use. We hope that modes for the onset of chain reactions can be calculated as a succession of eigenvalue problems. Critical phenomena should be tackled with further degrees of freedom, their traces cause an indeterminacy for states of rest.

In the long run transitions to and from granular fluids, suspensions and gases have to be considered in order to capture changing boundaries due to placement and removal (PSM).

Thermal activations should be considered in extensions of GSH. They can play a role even with hard grains in case of strong seismicity, and certainly with capillary bridges and soft grains. It could be of use to consider ductile solids with simultaneous seismic and thermal activation. This could help to support and substitute visco-hypoplastic relations in the validated range (PSM). Critical phenomena should embrace fracture by tension and shrinkage, this could help to establish fractals and strange attractors.

Appendix: Dimensionless GSH equations for triaxial tests

General GSH equations: We start with the following equations of motion neglecting thermal effects,

$$\partial_t \rho + \nabla_k (\rho v_k) = 0 \tag{64}$$
$$\partial_t (\rho v_i) + \nabla_k \sigma_{ik} = 0 \tag{65}$$
$$(\partial_t + v_k \nabla_k) u_{ij} = v_{ij} - u_{ik}\nabla_j v_k - u_{jk}\nabla_i v_k + X_{ij} \tag{66}$$
$$\partial_t s_g + \nabla_k \left(s_g v_k - f_k\right) = R_g/T_g - I, \tag{67}$$

the dissipative fluxes according to Onsager,

$$\begin{pmatrix} y_i \\ Y_{ij} \\ I \\ \sigma^{\mathrm{D}}_{ij} \end{pmatrix} = \begin{pmatrix} \beta_{ij} & 0 & 0 & 0 \\ 0 & \lambda_{ijlk} & 0 & -\alpha_{ijlk} \\ 0 & 0 & \gamma & 0 \\ 0 & \alpha_{lkij} & 0 & \eta_{ijlk} \end{pmatrix} \begin{pmatrix} \nabla_n \pi_{jn} \\ \pi_{lk} \\ T_g \\ v_{lk} \end{pmatrix} \tag{68}$$

$$\begin{pmatrix} f_i \\ \Sigma_{ij} \end{pmatrix} = \begin{pmatrix} \kappa_{ij} & 0 \\ 0 & \eta^{\mathrm{g}}_{ijlk} \end{pmatrix} \begin{pmatrix} \nabla_j T_g \\ v_{lk} \end{pmatrix}, \tag{69}$$

and the thermodynamic relations

$$\sigma_{ij} = \rho v_i v_j + P_T \delta_{ij} + \pi_{ij} - \sigma^{\mathrm{D}}_{ij} - \Sigma_{ij}, \tag{70}$$
$$R_g = f_k \nabla_k T_g + \Sigma_{ij} v_{ij}, \tag{71}$$
$$\pi_{ij} = -\frac{\partial F}{\partial u_{ij}}, \tag{72}$$
$$s_g = -\frac{\partial F}{\partial T_g}, \tag{73}$$
$$P_T = \left(\frac{\rho \partial}{\partial \rho} - 1\right) F, \tag{74}$$
$$X_{ij} = -\left(\nabla_j y_i + \nabla_i y_j\right)/2 + Y_{ij}. \tag{75}$$

These equations are closed once the expressions for the free energy F and the transport coefficients are given.

If we take the off-diagonal coefficients of the Onsager matrices as given in (68, 69), we have

$$y_i = \beta_{ij} \nabla_n \pi_{jn}, \tag{76}$$
$$Y_{ij} = \lambda_{ijlk} \pi_{lk} - \alpha_{ijlk} v_{lk}, \tag{77}$$
$$I = \gamma T_g, \tag{78}$$
$$\sigma^{\mathrm{D}}_{ij} = \alpha_{lkij} \pi_{lk} + \eta_{ijlk} v_{lk}, \tag{79}$$
$$\Sigma_{ij} = \eta^{\mathrm{g}}_{ijlk} v_{lk}, \tag{80}$$
$$f_i = \kappa_{ij} \nabla_j T_g. \tag{81}$$

So the stress tensor (70) becomes (neglecting the convective part $\rho v_i v_j$)

$$\sigma_{ij} = P_T \delta_{ij} + \pi_{ij} - \alpha_{lkij} \pi_{lk} - \left(\eta_{ijlk} + \eta^{\mathrm{g}}_{ijlk}\right) v_{lk}. \tag{82}$$

Equations (64–82) are the general scheme of GSH.

Triaxial tests: For simplicity we assume the samples is an element, i.e. density, stress, strain, deformation rate, etc. are all spatially uniform. Also, cylindrical symmetry is assumed. For the case of triaxial tests, the tensors u_{ij}, σ_{ij}, v_{ij} can be written as sums of isotropic and deviatoric parts:

$$u_{ij} = \frac{-\Delta}{3} \begin{pmatrix} 1 & 0 & 0 \\ 0 & 1 & 0 \\ 0 & 0 & 1 \end{pmatrix} + \frac{U}{3} \begin{pmatrix} -1 & 0 & 0 \\ 0 & -1 & 0 \\ 0 & 0 & 2 \end{pmatrix}, \tag{83}$$

$$\sigma_{ij} = P \begin{pmatrix} 1 & 0 & 0 \\ 0 & 1 & 0 \\ 0 & 0 & 1 \end{pmatrix} + \frac{q}{3} \begin{pmatrix} -1 & 0 & 0 \\ 0 & -1 & 0 \\ 0 & 0 & 2 \end{pmatrix}, \tag{84}$$

$$v_{ij} = \frac{-V}{3} \begin{pmatrix} 1\,0\,0 \\ 0\,1\,0 \\ 0\,0\,1 \end{pmatrix} + \frac{\Upsilon}{3} \begin{pmatrix} -1 & 0 & 0 \\ 0 & -1 & 0 \\ 0 & 0 & 2 \end{pmatrix}, \tag{85}$$

with the shear strain strength $u_s = \sqrt{2/3}\,|U|$, shear stress strength $\sigma_s = \sqrt{2/3}\,|q|$, shear deformation rate $v_s = \sqrt{2/3}\,|\Upsilon|$, etc.

The dissipative fluxes vanish, $y_i = 0$, $f_i = 0$, due to the assumption of spatial uniformity. The equation of motions (64–67) become

$$\partial_t \rho = \rho V, \tag{86}$$
$$\partial_t u_{ij} = v_{ij} - u_{ik}\nabla_j v_k - u_{jk}\nabla_i v_k + Y_{ij}, \tag{87}$$
$$\partial_t s_g - s_g V = R_g/T_g - I, \tag{88}$$

or, neglecting higher terms such as $u_{ik}\nabla_j v_k$,

$$\partial_t \rho = \rho V, \tag{89}$$
$$\partial_t \Delta = V - \lambda_{nnlk}\pi_{lk} + \alpha_{nnlk} v_{lk}, \tag{90}$$
$$\partial_t U - \Upsilon = (\lambda_{zzlk} - \lambda_{xxlk})\,\pi_{lk} - (\alpha_{zzlk} - \alpha_{xxlk})\,v_{lk}, \tag{91}$$
$$\partial_t \vartheta = \frac{\eta^{\mathrm{g}}_{ijlk}}{\rho T_g} v_{lk} v_{ij} - \frac{\gamma T_g}{\rho}, \tag{92}$$

if the dissipative fluxes (77–80) are inserted. Here $\vartheta \equiv s_g/\rho$ is the granular entropy per unit mass. Moreover, according to (82), the stresses P, q are

$$P = P_T + \frac{\pi_{nn}}{3} - \frac{\alpha_{lknn}\pi_{lk}}{3} - \left(\eta_{nnlk} + \eta^{\mathrm{g}}_{nnlk}\right)\frac{v_{lk}}{3}, \tag{93}$$

$$q = \pi_{zz} - \pi_{xx} - \left(\alpha_{lkzz} - \alpha_{lkxx}\right)\pi_{lk} - \left(\eta_{zzlk} - \eta_{xxlk} + \eta^{\mathrm{g}}_{zzlk} - \eta^{\mathrm{g}}_{xxlk}\right)v_{lk}. \tag{94}$$

Equations (89–91) are the basic equations for analyzing triaxial dynamics. They will be closed by material relations, i.e. expressions for the free energy and the transport coefficients.

Models: Next, consider the material relations. When without intrinsic (or fabric) anisotropy, the free energy has the form $F\left(\rho, T_g, u_{ij}\right) = F\left(\rho, T_g, \Delta, u_s, u_{III}\right)$ with $u_{III} \equiv \sqrt[3]{u^*_{ij}u^*_{jk}u^*_{ki}}$ the third strain invariant. We then have

$$\pi_{ij} = \pi_1\delta_{ij} + \pi_2 u^*_{ij} + \pi_3 u^{**}_{ij}, \quad \text{with} \tag{95}$$

$$\pi_1 = \frac{\partial F}{\partial \Delta}, \qquad \pi_2 = -\frac{1}{u_s}\frac{\partial F}{\partial u_s}, \tag{96}$$

$$\pi_3 = -\frac{1}{u^2_{III}}\frac{\partial F}{\partial u_{III}}, \tag{97}$$

where $u^{**}_{ij} \equiv u^*_{ik}u^*_{kj} - u^*_{kl}u^*_{kl}\delta_{ij}/3$ is the traceless part of the the deviatoric strain squared. We can further assume that the thermodynamic energy has the form

$$F = F_0\left(\rho, \Delta, u_s, u_{III}\right) - \frac{b}{2}\rho T_g^2, \tag{98}$$

$$b = b_0\left(1 - \widetilde{\rho}\right)^a, \tag{99}$$

where F_0 is an elastic potential, and

$$\widetilde{\rho} \equiv \rho/\rho_{cp} \tag{100}$$

a dimensionless density. This implies there is no coupling between elasticity and the granular entropy. The model gives

$$\vartheta = bT_g, \tag{101}$$

$$P_T = \frac{a}{2}\frac{b\rho^2 T_g^2}{\rho_{cp}\left(1 - \widetilde{\rho}\right)}, \tag{102}$$

where terms of order $\Delta^{2.5}$ in P_T are neglected. For isotropic material, the tensorial coefficients in (68,69) such as η_{ijlk} or α_{ijlk} can be written as

$$\alpha_{ijlk} = \alpha_1\delta_{ik}\delta_{lj} - \left(\alpha_1 - \alpha_2\right)\delta_{ij}\delta_{kl}/3, + \alpha_3\left(u^*_{ij}\delta_{kl} + \delta_{ij}u^*_{kl}\right) \tag{103}$$

$$\lambda_{ijlk} = -\frac{u_{ij}}{\tau}\frac{\pi^*_{lk}}{\pi^2_s} + \Delta\left(\frac{1}{\tau_1} - \frac{1}{3\tau}\right)\frac{\delta_{ij}\delta_{lk}}{\pi_{nn}}, \tag{104}$$

$$\eta_{ijlk} = \eta\delta_{il}\delta_{jk} + \left(\zeta - \frac{\eta}{3}\right)\delta_{ij}\delta_{lk}, \tag{105}$$

$$\eta^{\mathrm{g}}_{ijlk} = \eta_g\delta_{il}\delta_{jk} + \left(\zeta_g - \frac{\eta_g}{3}\right)\delta_{ij}\delta_{lk}. \tag{106}$$

Note that (104) is a relaxation time model for strain, with τ, τ_1 being two relaxation times.

Inserting the features of this model into the triaxial equations (89–92), we obtain the following governing equations for triaxial dynamics

$$\partial_t\rho = \rho V, \tag{107}$$

$$\partial_t\Delta = \left(1 - \alpha_2\right)V + 2\alpha_3 U\Upsilon - \frac{3}{\tau_1}\Delta, \tag{108}$$

$$\partial_t U = \left(1 - \alpha_1\right)\Upsilon + \alpha_3 VU - \frac{U}{\tau}, \tag{109}$$

$$\partial_t\vartheta = \frac{2}{3}\frac{b\eta_g}{\rho\vartheta}\Upsilon^2 + \frac{b\zeta_g}{\rho\vartheta}V^2 - \frac{\gamma}{b\rho}\vartheta, \tag{110}$$

and

$$P = P_T + \left(1 - \alpha_2\right)\pi_1 - \frac{2}{3}\alpha_3\left(\pi_2 + \pi_3\frac{U}{3}\right)U^2, + \left(\zeta + \zeta_g\right)V \tag{111}$$

$$q = \left[\left(1 - \alpha_1\right)\left(\pi_2 + \pi_3\frac{U}{3}\right) - 3\alpha_3\pi_1\right]U - \left(\eta + \eta_g\right)\Upsilon. \tag{112}$$

Here we used the facts that for the triaxial case $u^*_{ij}u^*_{ij} = u^2_s = 2U^2/3$ and $u^{**}_{ij} = Uu^*_{ij}/3$. So $\pi_{kk} = 3\pi_1$ and $u^*_{kl}\pi^*_{lk} = (2/3)\left(\pi_2 + \pi_3 U/3\right)U^2$ according to (95). Also $u^*_{kl}v^*_{lk} = 2U\Upsilon/3$ and $\eta^{\mathrm{g}}_{ijlk}v_{lk}v_{ij} = 2\eta_g\Upsilon^2/3 + \zeta_g V^2$ according to (106), $\lambda_{nnlk}\pi_{lk} = 3\Delta/\tau_1$ and $\left(\lambda_{zzlk} - \lambda_{xxlk}\right)\pi_{lk} = -U/\tau$ according to (95, 104), $\alpha_{nnlk}v_{lk} = 2\alpha_3 U\Upsilon - \alpha_2 V$ and $\left(\alpha_{zzlk} - \alpha_{xxlk}\right)v_{lk} = \alpha_1 U - \alpha_3 UV$ according to (103), $\alpha_{lknn}\pi_{lk} = 3\alpha_2\pi_1 + 2\alpha_3 U^2\left(\pi_2 + \pi_3 U/3\right)$ and $\left(\alpha_{lkzz} - \alpha_{lkxx}\right)\pi_{lk} = U\left[3\alpha_3\pi_1 + \alpha_1\left(\pi_2 + \pi_3 U/3\right)\right]$ according to (95, 103).

Algorithm: For solving the triaxial equations numerically, it will be convenient to introduce a characteristic time scale t_*. Writing $\gamma_0 = \gamma^*_0\widetilde{\gamma}_0$ with γ^*_0 a constant and $\widetilde{\gamma}_0$ a dimensionless factor which accounts for variation of γ_0 with density $\widetilde{\rho}$, we can define the time scale by

$$t_* = \frac{b_0\rho_{cp}}{\gamma^*_0}. \tag{113}$$

Furthermore, an entropy scale

$$\vartheta_* = \sqrt{\frac{B_0 b_0}{\rho_{cp}}}, \tag{114}$$

and a stress scale, B_0, can be also introduced. With help of these scales, the following dimensionless variables (denoted by $\widetilde{\ }$) will be used for numerical computations:

$$\widetilde{t} = \frac{t}{t_*}, \quad \widetilde{V} = t_* V, \quad \widetilde{\Upsilon} = t_*\Upsilon, \quad \widetilde{\vartheta} = \frac{\vartheta}{\vartheta_*}, \tag{115}$$

$$\widetilde{P} = \frac{P}{B_0}, \quad \widetilde{q} = \frac{q}{B_0}, \quad \widetilde{\pi}_{1,2,3} = \frac{\pi_{1,2,3}}{B_0}. \tag{116}$$

In these dimensionless variables, the Equations (107–112) become

$$\widehat{\widetilde{\rho}} = \widetilde{\rho}\widetilde{V}, \tag{117}$$

$$\widehat{\widetilde{\Delta}} = (1-\alpha_2)\,\widetilde{V} + 2\alpha_3 U\widetilde{\Upsilon} - \frac{3}{\widetilde{\tau}_1}\Delta, \tag{118}$$

$$\widehat{\widetilde{U}} = (1-\alpha_1)\,\widetilde{\Upsilon} + \alpha_3 U\widetilde{V} - \frac{U}{\widetilde{\tau}}, \tag{119}$$

$$\widehat{\widetilde{\vartheta}} = \frac{2}{3}\widetilde{\eta}_g\widetilde{\Upsilon}^2 + \widetilde{\zeta}_2\widetilde{V}^2 - \widetilde{\gamma}\widetilde{\vartheta}, \tag{120}$$

$$\widetilde{q} = \left[(1-\alpha_1)\left(\widetilde{\pi}_2 + \widetilde{\pi}_3\frac{U}{3}\right) - 3\alpha_3\widetilde{\pi}_1\right]U - \left(\widetilde{\eta} + \frac{\widetilde{\rho}\widetilde{\vartheta}\widetilde{\eta}_g}{(1-\widetilde{\rho})^a}\right)\widetilde{\Upsilon}, \tag{121}$$

$$\widetilde{P} = \frac{a}{2}\frac{\widetilde{\rho}^2\widetilde{\vartheta}^2}{(1-\widetilde{\rho})^{1+a}} + (1-\alpha_2)\,\widetilde{\pi}_1 - \frac{2}{3}\alpha_3\left(\widetilde{\pi}_2 + \widetilde{\pi}_3\frac{U}{3}\right)U^2 + \left(\widetilde{\zeta} + \frac{\widetilde{\rho}\widetilde{\vartheta}\widetilde{\zeta}_g}{(1-\widetilde{\rho})^a}\right)\widetilde{V}. \tag{122}$$

Here the quantities with $\widehat{\ }$ are

$$\widehat{\widetilde{\rho}} = \widetilde{\partial}_t\widetilde{\rho}, \quad \widehat{\widetilde{\Delta}} = \widetilde{\partial}_t\Delta, \quad \widehat{\widetilde{U}} = \widetilde{\partial}_t U, \quad \widehat{\widetilde{\vartheta}} = \widetilde{\partial}_t\widetilde{\vartheta} \tag{123}$$

where $\widetilde{\partial}_t$ is derivative with $\widetilde{t}$. The dimensionless coefficients are

$$\widetilde{\eta}_g\left(\widetilde{\rho},\widetilde{\vartheta}\right) = \frac{b\eta_g}{t^*\vartheta_*\rho\vartheta}, \tag{124}$$

$$\widetilde{\zeta}_g\left(\widetilde{\rho},\widetilde{\vartheta}\right) = \frac{b\zeta_g}{t^*\vartheta_*\rho\vartheta}, \tag{125}$$

$$\widetilde{\gamma}\left(\widetilde{\rho},\widetilde{\vartheta}\right) = \frac{t^*\gamma}{b\rho}, \tag{126}$$

$$\widetilde{\tau}\left(\widetilde{\rho},\widetilde{\vartheta}\right) = \tau/t^*, \tag{127}$$

$$\widetilde{\tau}_1\left(\widetilde{\rho},\widetilde{\vartheta}\right) = \tau_1/t^*, \tag{128}$$

and

$$\widetilde{\eta} = \frac{\eta}{B_0 t^*}, \tag{129}$$

$$\widetilde{\zeta} = \frac{\zeta}{B_0 t^*}. \tag{130}$$

In computations, the evolution of the 12 triaxial variables

$$\left\{\widetilde{\rho}_0, \widetilde{\Delta}_0, \widetilde{U}_0, \widetilde{\vartheta}_0, \widetilde{V}_0, \widetilde{\Upsilon}_0, \widetilde{P}_0, \widetilde{q}_0, \widehat{\rho}_0, \widehat{\Delta}_0, \widehat{U}_0, \widehat{\vartheta}_0\right\} \tag{131}$$

after a time step $d\widetilde{t}$ can be calculated by solving the Equations (117–122) and the discrete forms of (123):

$$\widetilde{\rho} = \widetilde{\rho}_0 + \left(\widehat{\rho} + \widehat{\rho}_0\right)\frac{d\widetilde{t}}{2}, \tag{132}$$

$$\widetilde{\Delta} = \widetilde{\Delta}_0 + \left(\widehat{\Delta} + \widehat{\Delta}_0\right)\frac{d\widetilde{t}}{2}, \tag{133}$$

$$\widetilde{U} = \widetilde{U}_0 + \left(\widehat{U} + \widehat{U}_0\right)\frac{d\widetilde{t}}{2}, \tag{134}$$

$$\widetilde{\vartheta} = \widetilde{\vartheta}_0 + \left(\widehat{\vartheta} + \widehat{\vartheta}_0\right)\frac{d\widetilde{t}}{2}. \tag{135}$$

in

$$\left\{\widetilde{\rho}, \widetilde{\Delta}, \widetilde{U}, \widetilde{\vartheta}, \widetilde{V}, \widetilde{\Upsilon}, \widetilde{P}, \widetilde{q}, \widehat{\rho}, \widehat{\Delta}, \widehat{U}, \widehat{\vartheta}\right\}. \tag{136}$$

Because of the symmetry of triaxial tests, two temporal evolutions determining any of $\widetilde{V}, \widetilde{\Upsilon}, \widetilde{P}, \widetilde{q}$ (or their combinations) are sufficient. Therefore, the ten Eqs. (117–122,132–135) fully determine the dynamics.

In the present work, we take the elastic potential to be

$$F_0 = B_0\widetilde{B}\sqrt{\Delta}\left(\frac{2}{5}\Delta^2 + \frac{1}{\xi}u_s^2\right), \tag{137}$$

$$\widetilde{B} = \left(\frac{\widetilde{\rho}-\rho_1}{1-\widetilde{\rho}}\right)^{0.15}, \tag{138}$$

with $B_0 = 7\,\mathrm{GPa}$, $\xi = 5/3$, which leads to

$$\widetilde{\pi}_1 = \widetilde{B}\Delta\sqrt{\Delta}\left(1 + \frac{1}{3\xi}\frac{U^2}{\Delta^2}\right), \tag{139}$$

$$\widetilde{\pi}_2 = -\frac{2}{\xi}\widetilde{B}\sqrt{\Delta}, \tag{140}$$

and $\widetilde{\pi}_3 = 0$. The transport coefficients will be modeled as

$$\tau^{-1} = \lambda T_g, \tag{141}$$

$$\tau_1^{-1} = \lambda_1 T_g, \tag{142}$$

$$\eta_g = \eta_0 + \eta_1 T_g, \tag{143}$$

$$\zeta_g = \zeta_0 + \zeta_1 T_g, \tag{144}$$

$$\gamma = \gamma_0 + \gamma_1 T_g, \tag{145}$$

with λ, λ_1, $\eta_{0,1}$, $\zeta_{0,1}$, $\gamma_{0,1}$ density dependent factors. According to (124–128), we therefore have

$$\widetilde{\eta}_g = \frac{b\eta_0}{t^*\vartheta_*^2\rho\widetilde{\vartheta}} + \frac{\eta_1}{t^*\vartheta_*\rho}, \tag{146}$$

$$\widetilde{\zeta}_g = \frac{b\zeta_0}{t^*\vartheta_*^2\rho\widetilde{\vartheta}} + \frac{\zeta_1}{t^*\vartheta_*\rho}, \tag{147}$$

$$\widetilde{\gamma} = \frac{t^*\gamma_0}{b\rho} + \frac{t^*\vartheta_*\gamma_1}{b^2\rho}\widetilde{\vartheta}, \tag{148}$$

$$\widetilde{\tau} = \frac{b}{\vartheta_* t^*\lambda\widetilde{\vartheta}}, \tag{149}$$

$$\widetilde{\tau}_1 = \frac{b}{\vartheta_* t^*\lambda_1\widetilde{\vartheta}}. \tag{150}$$

References

1. Jaeger, H.M., Nagel, S.R., Behringer, R.P.: Granular solids, liquids, and gases. Rev. Mod. Phys. **68**(4), 10 (1996)
2. Darwin, G.H.: On the horizontal thrust of a mass of sand. In: Minutes Proceedings Inst. Civ. Eng., pp. 350–378 (1983)
3. Matsushita, M., Tatsuoka, F., Koseki, J., Cazacliu, B., di Benedetto, H., Yasin, S.J.M.: Time effects on the pre-peak deformation properties of sands. In: International Conference Pre-Failure Deformation Characteristics of Geomaterials, pp. 681–689 (1999)
4. Gudehus, G., Goldscheider, M., Winter, H.: Mechanical Properties of Sand and Clay and Numerical Integration Methods: Some

Sources of Errors and Bounds of Accuracy, pages 121–150 Balkema, (1977)
5. Gudehus, G.: Seismo-hypoplasticity with a granular temperature. Granular Matter **8**(2), 93–102 (2006)
6. Niemunis, A.: Extended hypoplastic models for soils. Polytechnica, Gdansk (2003)
7. Barkan, D.D.: Dynamics of Bases and Foundations. McGraw-Hill Book Company, New York (1962)
8. Valanis, K.C., Peters, J.F., Gill, J.: Configurational entropy, non-associativity and uniqueness in granular media. Acta Mechanica, p. 100. (1993)
9. Herrmann, H.J.: On the thermodynamics of granular media. J. Phys. II France **3**, 427–433 (1993)
10. Edwards, S.F., Oakeshott, R.B.S.: Granular matter: An interdisciplinary approach. Phys. A **157**, (1989)
11. Kondic, L., Behringer, R.P.: Elastic energy, fluctuations and temperature for granular materials. Europhys. Lett. **67**(2), 205–211 (2004)
12. Landau, L.D., Lifshitz, E.M.: Fluid Mechanics. Butterworth-Heinemann, Oxford (1987)
13. Landau, L.D., Lifshitz, E.M.: Theory of Elasticity. Butterworth-Heinemann, Oxford (1986)
14. Khalatnikov, I.M.: Introduction to the Theory of Superfluidity. Benjamin, New York (1965)
15. de Groot, S.R., Masur, P.: Non-Equilibrium Thermodynamics. Dover, New York (1984)
16. de Gennes, P.G., Prost, J.: The Physics of Liquid Crystals. Clarendon Press, Oxford (1993)
17. Müller, H.W., Liu, M.: Structure of ferro-fluiddynamics. Phys. Rev. E **64**, 061405 (2001)
18. Müller, O., Hahn, D., Liu, M.: Non-Newtonian behaviour in ferrofluids and magnetization relaxation. J. Phys. Condens. Matter **18**, 2623 (2006)
19. Temmen, H., Pleiner, H., Liu, M., Brand, H.R.: Convective nonlinearity in non-Newtonian fluids. Phys. Rev. Lett. **84**(15), 3228–3231 (2000)
20. Müller, O.: Die Hydrodynamische Theorie Polymerer Fluide. PhD thesis, University of Tübingen (2006)
21. Kadanoff, L.P.: Built upon sand: theoretical ideas inspired by granular flows. Rev. Mod. Phys. **71**(1), 435–444 (1999)
22. Jiang, Y., Liu, M.: Granular elasticity without the Coulomb condition. Phys. Rev. Lett. **91**(14), 144301 (2003)
23. Jiang, Y., Liu, M.: Energetic instability unjams sand and suspension. Phys. Rev. Lett **93**(14), 148001 (2004)
24. Jiang, Y., Liu, M.: A brief review of granular elasticity. Eur. Phys. J. E Soft Matter **22**(3), 255 (2007)
25. Jiang, Y., Liu, M.: From elasticity to hypoplasticity: dynamics of granular solids. Phys. Rev. Lett **99**(10), 105501 (2007)
26. Jiang, Y., Liu, M.: Granular solid hydrodynamics. Granular Matter **11**, 139 (2009)
27. Jiang, Y., Liu, M.: The physics of granular mechanics. In: Kolymbas, D., Viggiani, G. (eds.) Mechanics of Natural Solids, pp. 27–46. Springer, Berlin (2009)
28. Guyon, E., Troadec, J.P.: Du sac de billes au tas de sable. Odile Jacob, Paris (1994)
29. Pacheco-Martinez, H., Jan van Gerner, H., Ruiz-Suárez, J.C.: Storage and discharge of a granular fluid. Phys. Rev. E **77**, 021303 (2008)
30. Pöschel, Th., Luding, St.: Granular Gases. Springer, Berlin (2001)
31. Huber, G., Wienbroer, H.: Vibro-viscosity and granular temperature of cylindrical grain skeletons-experiments. In: Herrmann, H., Garcia-Rojo, R., McNamara, S., (eds.) Powders and Grains 05, p. 287–290 (2005)
32. Luong, M.P.: Mechanical aspects and thermal effects of cohesionless soils under cyclic and transient loading. In: Proceedings of IUTAM Conference on Deformation and Failure of Granular Materials, pp. 239–246 Delft (1982)
33. Kolymbas, D., Wu, W.: Introduction to hypoplasticity. In: Kolymbas, D. (ed.) Modern Approaches to Plasticity, pp. 213–224. Elsevier, Amsterdam (1983)
34. Wu, W., Bauer, E.: A hypoplastic model for barotropy and pyknotropy of granular soils. In: Kolymbas, D. (ed.) Modern Approaches to Plasticity, pp. 225–246. Elsevier, Amsterdam (1983)
35. Tatsuoka, F., Di Benedetto, H., Enomoto, T., Kawabe, S., Kongkitkul, W.: Various viscosity types of geomaterials in shear and their mathematical expression. Soils Found **48**(1), (2008)
36. Huber, G.: Asymptotic beaviour of sand in resonant-column tests. Granular Matter (2010) (under preparation)
37. Youd, T.L.: Compaction of sands by repeated shear straining. In: Journal of Soil Mechanical and Found Engineering Division, ASCE, vol. 7, pp. 709–725 (1972)
38. Wichtmann, L., Niemunis, A., Triantafyllidis, T.: On the determination of a set of material constants for a high-cycle accumulation model for non-cohesive soils. Int. J. Numer. Anal. Meth. Geomech. (2009) (submitted)
39. Wichtmann, T., Niemunis, A., Triantafyllidis, T.: Experimental evidence of a unique flow rule of non-cohesive soils under high-cyclic loading. Acta Geotechnica **1**, 59–73 (2006)
40. Niemunis, A., Wichtmann, T., Triantafyllidis, Th.: A high-cycle accumulation model for sand. Comput. Geotech. **2**(4), 245–263 (2005)
41. Wichtmann, T.: *Explicit accumulation model for non-cohesive soils under cyclic loading. PhD thesis, Institut Grundbau und Bodenmech. Ruhr-Univ., Bochum, Germany, Heft 38 (2005)*
42. Ibsen, L.B.: The stable state in cyclic triaxial testing on sand. Soil Dyn. Earthq. Eng. **13**, 63–72 (1994)
43. Niemunis, A., Prada, A.: Lessons from fe implementation of sanisand and hypoplasticity. (2010) (in preparation)
44. Sturm, H.: Stabilisation behaviour of cyclically loaded shallow foundations for offshore wind turbines. PhD thesis, University of Karlsruhe (2009)
45. N. Triantafyllidis: Dynamic stiffness of rigid rectangular foundations on the half-space. Earthqu. Eng. Struct. Dyn. **14**, 391–411 (1986)
46. Rebstock, D.: Stressing and relaxation of sand. PhD thesis, Institute of Soil Mechanics and Rock Mechanics, University of Karlsruhe (2009)